

MICROCOMPUTER-CONTROLLED SERVO SYSTEM
FOR AN ULTRASONIC
COMPUTER-ASSISTED TOMOGRAPHIC SCANNER

BY

BENJAMIN LERNER

B.S., University of Illinois, 1975

THESIS

Submitted in partial fulfillment of the requirements
for the degree of Master of Science
in Electrical Engineering
in the Graduate College of the
University of Illinois at Urbana-Champaign, 1979

Urbana, Illinois

UNIVERSITY OF ILLINOIS
Urbana-Champaign Campus
The Graduate College
330 Administration Building

FORMAT APPROVAL

To the Graduate College:

The format of the thesis submitted by Benjamin Lerner
for the degree of Master of Science is acceptable to the
department of Electrical Engineering.

May 11, 1979

Date

(Signed)

Paul E. Maye
Departmental Representative

UNIVERSITY OF ILLINOIS AT URBANA-CHAMPAIGN

THE GRADUATE COLLEGE

MAY, 1979

WE HEREBY RECOMMEND THAT THE THESIS BY

BENJAMIN LERNER

ENTITLED MICROCOMPUTER-CONTROLLED SERVO SYSTEM FOR AN

ULTRASONIC COMPUTER-ASSISTED TOMOGRAPHIC SCANNER

BE ACCEPTED IN PARTIAL FULFILLMENT OF THE REQUIREMENTS FOR

THE DEGREE OF MASTER OF SCIENCE

William D. Bivin, Jr.

Michael S. Skonover
Director of Thesis Research

K. W. Brunt
Head of Department

Committee on Final Examination†

Chairman

† Required for doctor's degree but not for master's.

MICROCOMPUTER-CONTROLLED SERVO SYSTEM
FOR AN ULTRASONIC
COMPUTER-ASSISTED TOMOGRAPHIC SCANNER

BY

BENJAMIN LERNER

B.S., University of Illinois, 1975

THESIS

Submitted in partial fulfillment of the requirements
for the degree of Master of Science
in Electrical Engineering
in the Graduate College of the
University of Illinois at Urbana-Champaign, 1979

Urbana, Illinois

ACKNOWLEDGMENT

I wish to express my thanks and appreciation to Professor William D. O'Brien, Jr. of the Bioacoustics Research Laboratory and Professor Michael S. Schlansker of the Coordinated Science Laboratory at the University of Illinois for being my advisors on this project and for giving me the support and encouragement needed to make this project a success. I further wish to thank the numerous professors and graduate students with whom I have consulted while engaged in this project. Their help and advice, in disciplines ranging from control theory to bioengineering, has been most beneficial to carrying out the work described herein.

TABLE OF CONTENTS

CHAPTER

I	INTRODUCTION	1
II	DESIGN CONSTRAINTS	3
III	GENERAL CONTROLLER DESCRIPTION	11
IV	OVERVIEW OF VELOCITY & POSITION CONTROL.	14
V	MODEL OF ARMATURE-CONTROLLED DC MOTOR.	20
VI	ANALYSIS AND DESIGN OF A VELOCITY CONTROL SYSTEM	25
VII	STATE FEEDBACK WITH FULL-ORDER OBSERVER.	33
VIII	DISCRETE IMPLEMENTATION OF VELOCITY CONTROL. . .	37
IX	POSITIONAL CONTROL	47
APPENDIX		
A	SHAFT POSITION SENSING	54
B	PULSED MOTOR CONTROL	58
C	NUMERICAL CONSTANTS.	65
D	SYSTEM PERFORMANCE	70
E	PROGRAM LISTING.	73
REFERENCES	90

CHAPTER I

INTRODUCTION

Computer-Assisted Tomography, commonly known as "CAT Scanning", is the process of reconstructing a cross-sectional image, or tomogram, of a biological sample by using a digital computer to analyze a beam of radiation that is transmitted through the sample. The only commercial CAT scanners presently available transmit ionizing radiation (X-rays) and analyze their intensity after they pass through the sample.

The first CAT scanner to use ultrasonic radiation (sound waves at a higher frequency than the audible spectrum) was built at Mayo Clinic at Rochester, Minnesota. It is used primarily to scan women's breasts for cancerous tumors.

From the way ultrasound is believed to interact with biological tissue it is thought that ultrasonic CAT scanning (UCAT) can be used to extract information about the constituent properties of the tissue.

The Bioacoustics Research Laboratory at the University of Illinois at Urbana-Champaign has a grant from the National Institutes of Health's National Institute of General Medical Sciences (GM24994) to investigate new techniques of UCAT and to determine tissue constituent properties with ultrasound. One of the first parts of the project is to build an ultrasonic CAT scanner similar to the one at Mayo. It is from this aspect of the project that this paper developed, dealing with the

development of a computer-based controller for the ultrasonic
CAT scanner.

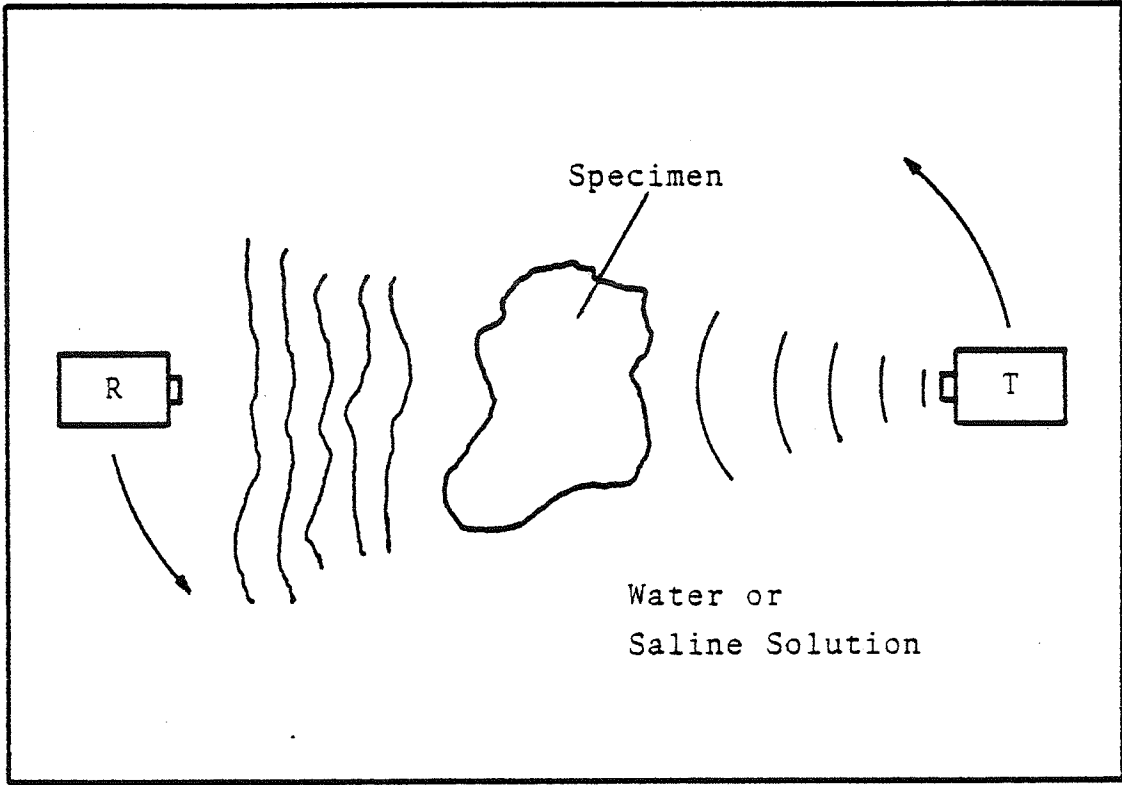
CHAPTER II

DESIGN CONSTRAINTS

Based upon extensive developmental work by Mayo Clinic engineers and scientists^[1-4] and upon our evaluation of their scanner design for our research requirements, a modified scanner has been designed. The aim was to be compatible with the system at Mayo Clinic and to satisfy our requirements.

Figure 1 shows the basic scanner concept. The scanner consists of a tank filled with a liquid in which the object to be scanned is suspended. On opposite sides of the object the ultrasonic transducers are mounted, in such a way that they can be revolved around the specimen. One of the transducers will always act as the transmitter, the other as the receiver. During the scanning process the transducers will be revolved around the specimen while the transmitter produces pulses of ultrasound. The receiver will receive the pulses after they pass through the specimen and the received signal will go to a digital computer for processing.

The transducers do not revolve around the specimen with a simple, continuous motion (Figure 2). The basic transmitter-receiver frame is positioned to an angle α with respect to the specimen. With α held constant, the receiver is moved through an angle 2β at a constant velocity, receiving the ultrasonic pulses that have been scattered to various angles by the specimen. This motion of the receiver is known as the "fan beam",



T - ULTRASONIC TRANSMITTER

R - ULTRASONIC RECEIVER

Figure 1. Ultrasonic Scanner Concept.

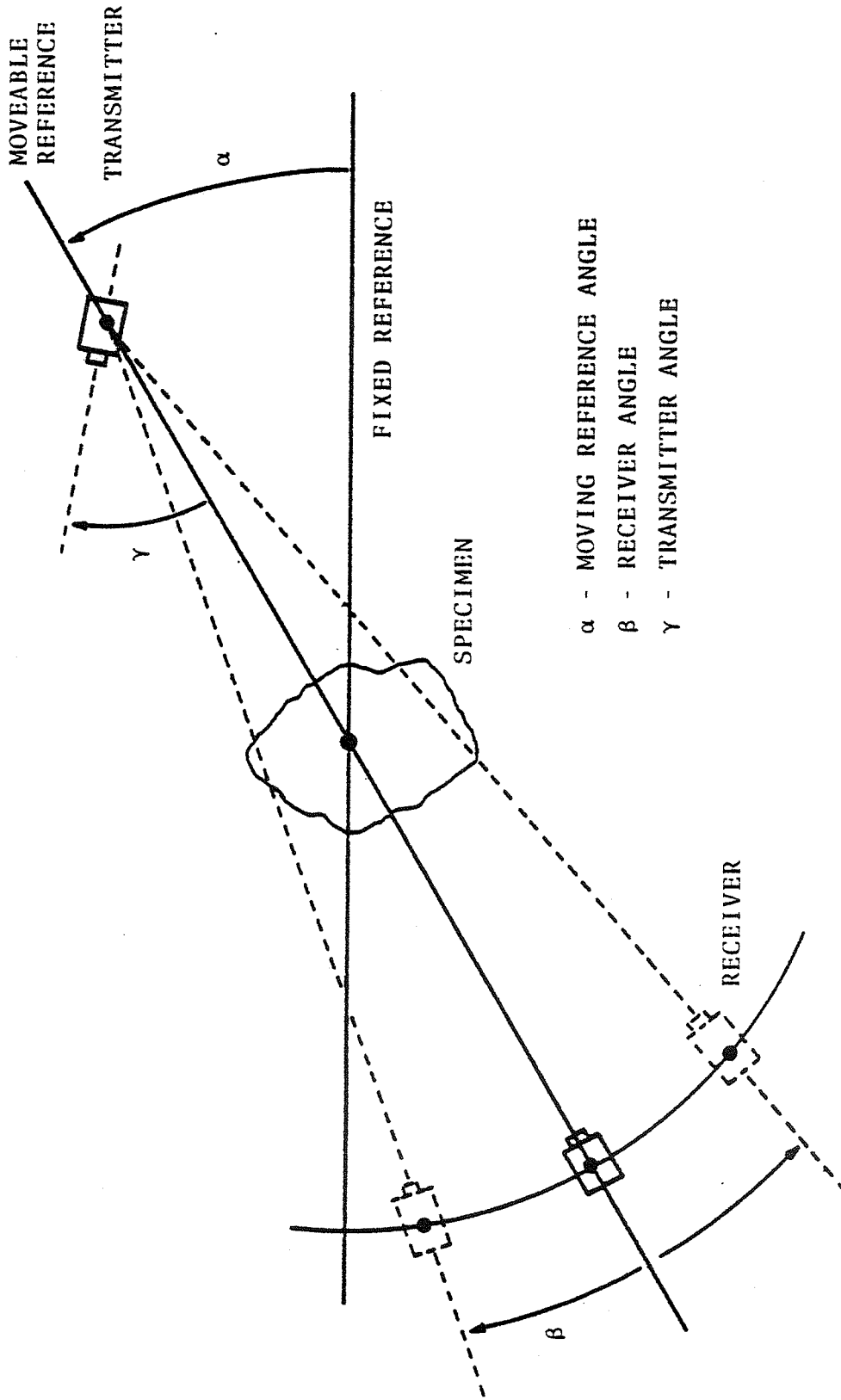


Figure 2. Transducer Motion.

and β is the fan-beam angle. When the fan-beam motion is complete, the receiver is halted and the entire transmitter-receiver frame is stepped through a small angle $\Delta\alpha$, typically 1° . The fan-beam motion is then reversed, and the receiver is moved through an angle of 2β in the opposite direction, while receiving scattered pulses from the specimen. This process is repeated until α has been moved across 180° . Because of symmetry it is not necessary to move across 360° .

The position of the receiver cannot be held constant with respect to the transmitter because the computer-algorithms that reconstruct the tomogram require pulse-transmission information through several angles of the specimen for a given reference angle α . There are two ways this information will be acquired, each requiring a different pivotal motion of the transmitter around its own axis (angle γ). During one type of data acquisition, $\gamma = \beta$ at all times so that the transmitter always points directly at the receiver. For the other type, the transmitter is pivoted to a given position and held there (γ is constant) while the receiver is swept through the fan-beam angle, 2β . It should be noted that the angles β and γ are taken relative to the moving reference-frame. The position of the moving reference frame is α , and is taken relative to the fixed reference frame, as shown in Figure 2.

It has been shown that the transducers have three degrees of freedom. Degree 1 is motion through the angle α , of the basic transmitter-receiver orientation. Degree 2 is the freedom

of the receiver to move through the angle β . Degree 3 is the freedom of the transmitter to be pivoted to any angle γ , on its own axis. There is a fourth degree of freedom in the scanner, which is the ability to move the specimen up and down relative to the height of transducers, which is fixed. This allows the transducers to scan successive cross-sections of the specimen.

Each degree of freedom will need to be powered by an electric motor. A major design decision was to decide whether to use DC motors or stepping motors. A stepping motor would be most suited to the 1st degree of freedom, since it involves motion of discrete increments, $\Delta\alpha$. The 2nd degree of freedom would be most easily served by a DC motor, since it requires smooth motion over a considerable distance. Due to the nature of the gear linkages in the scanner, the 3rd degree of freedom is also best served by a DC motor. For purposes of generality, and to simplify the system's control structure, it was decided to use the same type of motor throughout the scanner. The scanner requires a controller that will accept commands from the main computer to start a scan or move to a given position. The controller will control the application of power to the motors to carry out these commands. If all the motors are of the same type the job of the controller is simplified.

In the original scanner developed at Mayo Clinic, stepping motors are used. There are several problems with using stepping motors that were determined at Mayo as a result of their experience. A stepping motor is a discrete motion device and

many successive steps must be used to move the receiver through the fan-beam angle. At every step the motor starts and stops with a jerk. All of these jerks introduce vibration into the transducers. One of the measurements that is taken during a scan is the time-of-flight (TOF) of a pulse from transmitter to receiver, which is very sensitive to vibration. To decrease the vibration, Mayo developed a way of producing smooth, continuous motion with a stepping motor by varying the current through its coils in a sine-cosine pattern. With their experience it was decided against this approach because it involves taking a discrete-motion device, the stepping motor, and attaching it to a complex system to allow it to move smoothly. Since the system requires smooth motion, a DC motor was used from the start.

In choosing to use DC motors it became necessary to design a positioning system to allow the transducers to be stepped through α in increments $\Delta\alpha$. This would have been easier to do directly with a stepper motor, but this way the system gained the generality of a uniform control algorithm for all motors. The system now possesses the flexibility to step through the angle β while moving continuously through α , should a future experiment require it.

As was mentioned briefly before, the scanner must be able to receive commands from the main computer, a Perkin-Elmer 7/32. The commands will instruct the scanner where to move the transducers in the course of a scan. A control unit had to be de-

signed for the scanner, in order to receive the commands from the computer and control the motors to carry them out. It also must be able to transmit status information back to the 7/32. It was decided that the most flexible controller would be a microprocessor. It would require the least amount of special-purpose hardware, and design improvements could be achieved simply by modifying the software. This is illustrated in Figure 3.

To this point a description of the tomography project has been presented, followed by the design constraints for the ultrasonic scanner. The project described herein is to analyze and solve the problem of controlling the DC-motors in the scanner.

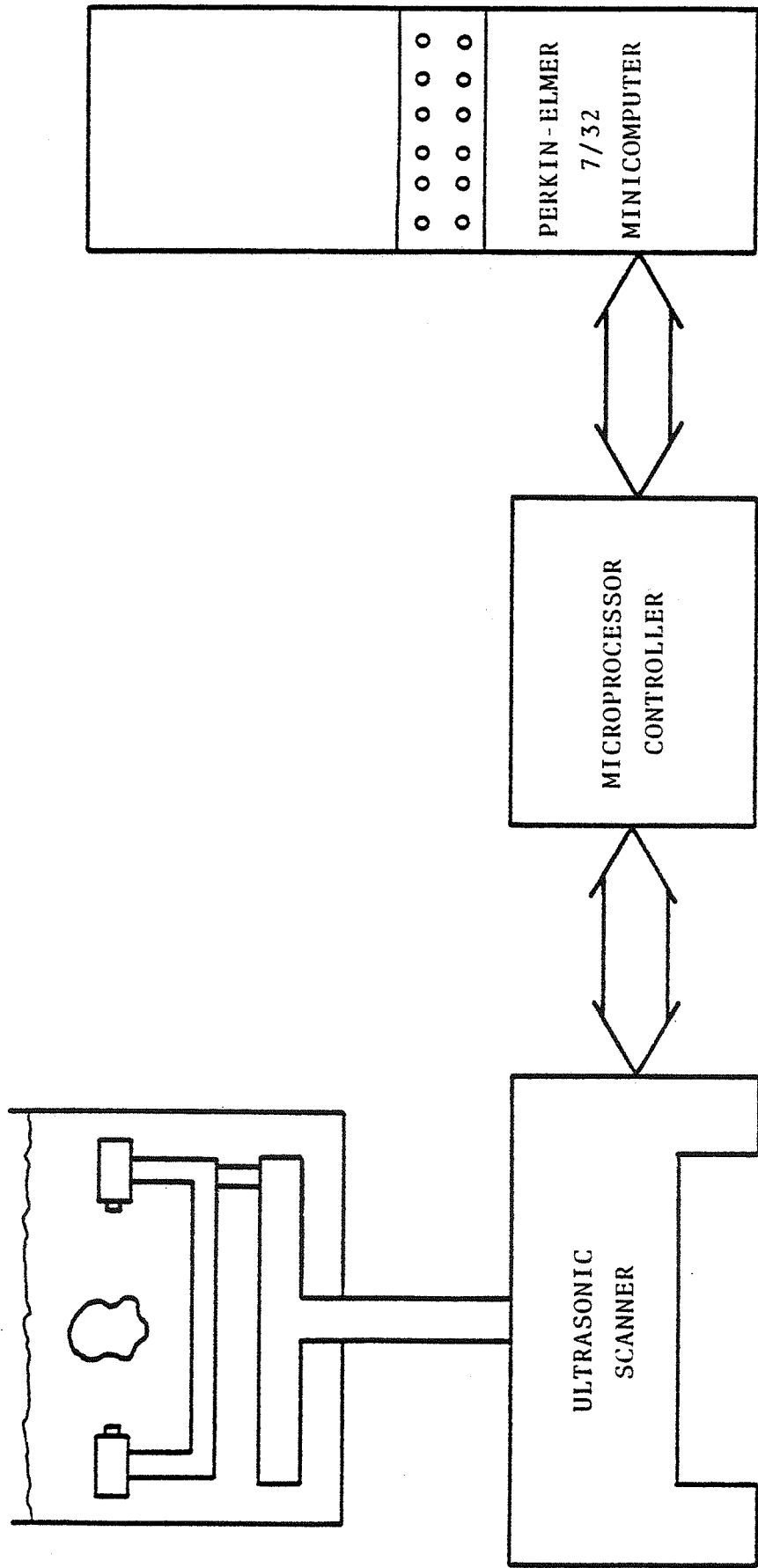


Figure 3. System Layout.

GENERAL CONTROLLER DESCRIPTION

The scanner's controller is a microprocessor that is programmed to accept commands from the 7/32 computer and control the scanner's motors in real-time to carry out those commands. It also must transmit information about the position of the transducers back to the 7/32, and is represented in a block diagram in Figure 4. The controller is implemented on a MOS Technology 6502 microprocessor. This processor was chosen because it has a very flexible instruction set [5] and an inexpensive microcomputer system utilizing this processor is available on the market [6]. This system consists of a single circuit board containing the processor, memory, input-output ports, and a sophisticated monitor program. It provides adequate software support to be usable as a self-contained development system, yet is sufficiently inexpensive to be dedicated as the controller.

The bulk of the software in the controller makes up a real-time, discrete "P-I-D" (Proportional-Integral-Differential) control algorithm [7] to control the motors. Feedback to the controller is by way of a shaft-encoder, a device that outputs a pulse for every given increment of a shaft's rotation. The encoder is mounted to provide position and velocity of the degrees of freedom. There is a separate encoder for each motor (see Appendix A).

The motors are controlled by a pulsed voltage. The pulse

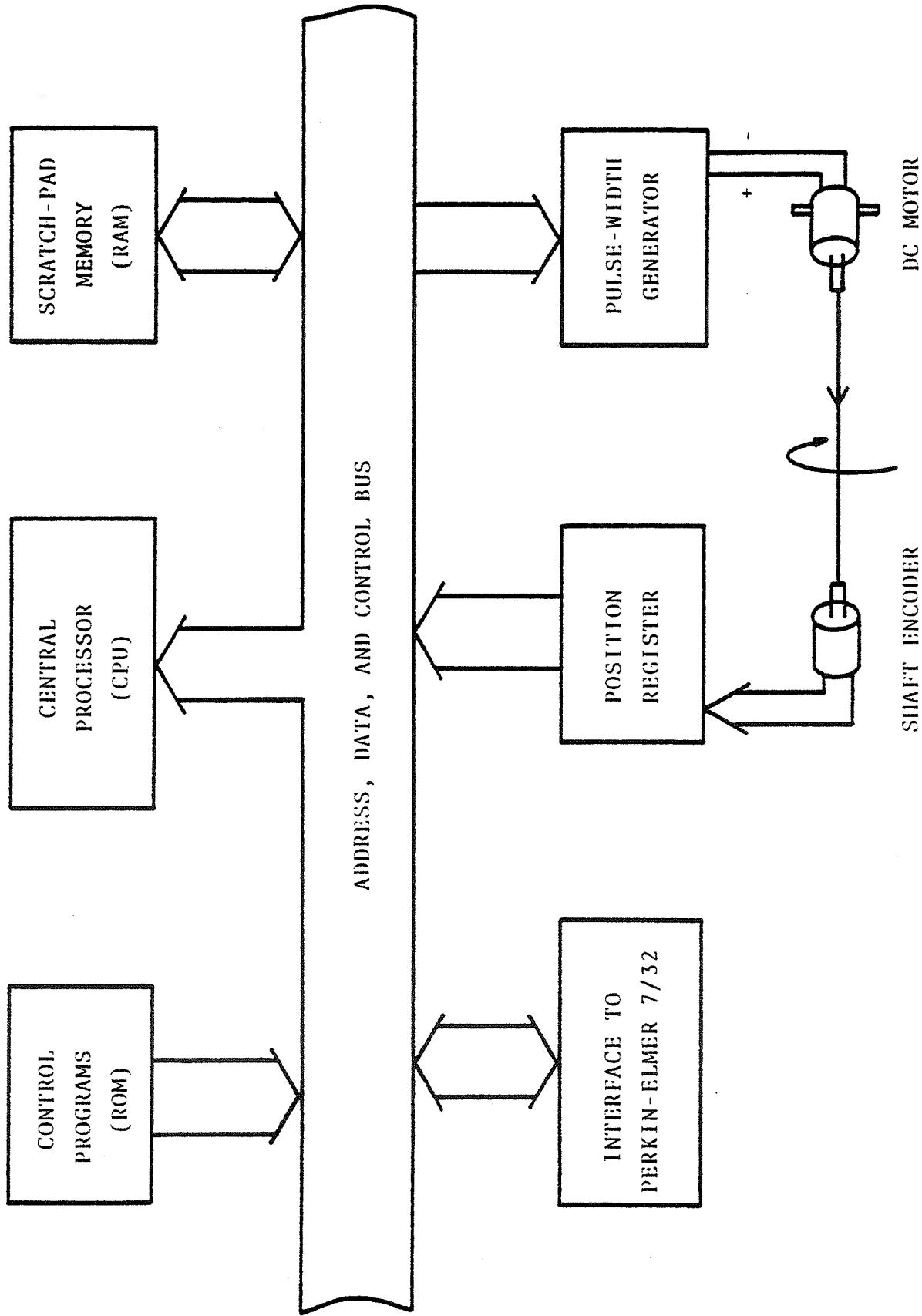


Figure 4. Microprocessor-Controller Block Diagram.

repetition frequency is fixed and the effective voltage is determined by the length of the duty cycle (see Appendix B). The controller outputs a control byte to the Pulse Width Generator (PWG), which causes it to send voltage pulses to the motor whose "ON" time is proportional to the value in the control byte. This method of control is advantageous because the final driver transistors are either off or saturated, so they do not dissipate as much power as they would if they were driven by a digital to analog converter and were operated in their linear region. The disadvantage to this approach is that by rapidly switching the power to the motor, a radio frequency interference (RFI) is caused which may interfere with the sensitive signal processing circuits that process the received ultrasonic signal. Should this become a problem, the PWG could be replaced with a digital to analog converter (DAC) and a power amplifier.

CHAPTER IV

OVERVIEW OF VELOCITY & POSITION CONTROL

The real-time controller will implement a velocity and position controller for a DC motor. An analysis of this problem follows.

Figure 5 is a block diagram of a basic velocity control system for a DC motor. The motor has an input voltage, V_m , and an output shaft velocity, ω_m . The problem at hand is to request a velocity, ω_r , and automatically control V_m so that the motor shaft turns at the rate ω_r . We wish for this to hold true even for fluctuations in the load on the motor. This is accomplished by feeding back ω_m and comparing it with ω_r . The difference between these velocities is the error velocity, denoted by ω_e . This error is the input to the controller. As long as the error is zero, the controller knows it is outputting the correct V_m . If ω_e deviates from zero due to, say, a variation in the motor's load or any other perturbation, the controller must adjust V_m to correct the speed of the motor.

A velocity control loop is the inner part of a position controller (Figure 6). The controller is given a request to move to a specific angle, θ_r . It computes the difference between the requested angle and the motor's present angle, θ_m . This is the angular error, θ_e . If θ_e is zero, the motor is positioned correctly and is not to move. If θ_e is non-zero, the position controller must request the velocity controller to

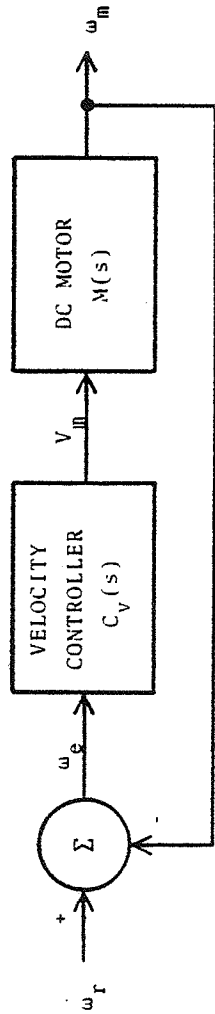


Figure 5. Velocity Control Block Diagram.

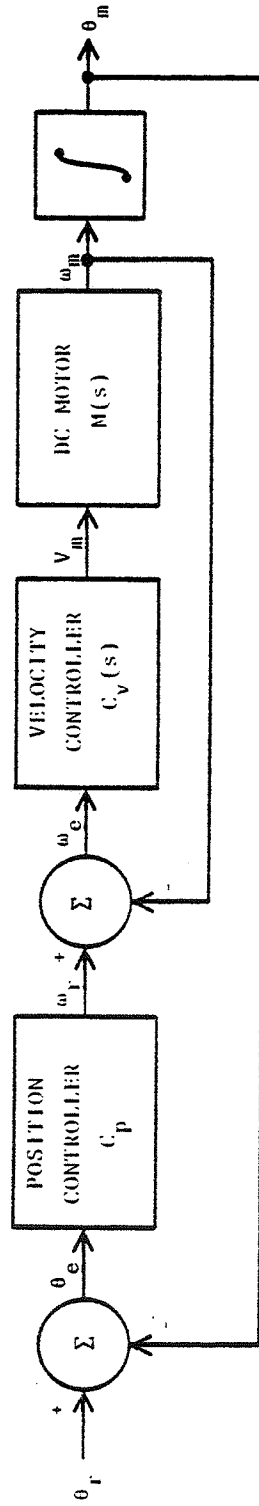


Figure 6. Position Control Block Diagram.

move the motor in the direction that will cause θ_e to decrease to zero. This is most simply done by letting $\omega_r = C_p \theta_e$ where C_p is the positional-control feedback constant. When the motor is in position, ω_r is zero. If the motor is ahead of or behind the requested position, a negative or positive velocity will be requested in proportion to θ_e . (C_p is assumed positive for this example.) As θ_e decreases, ω_r decreases with it.

Although the feedback for position control can be implemented by a constant gain (C_p), velocity control is not so simple. If a simple constant gain were used as feedback for velocity control, the motor voltage would be determined by $V_m = K_p \omega_e$. The subscript 'P' stands for 'proportional', since this is known as proportional control. If ω_e becomes zero V_m also becomes zero and the motor loses speed. An equilibrium point will be reached where the motor's velocity will be less than ω_r by enough so that V_m can keep the motor's speed constant. The error ω_e will never become zero. At equilibrium, ω_e is known as the steady-state error, e_{ss} . It is possible to decrease e_{ss} by increasing K_p , and

$$\lim_{K_p \rightarrow \infty} e_{ss} = 0$$

There are practical limitations to this, however, since the noise-sensitivity of the system, its sensitivity to random disturbances, is increased with K_p .

The solution to the problem of having steady-state error is to feed back the integral of the velocity error. Then the feedback expression becomes

$$V_m(t) = K_p \omega_e(t) + K_I \int_0^t \omega_e(\tau) d\tau. \quad (1)$$

' K_I ' is the integral-control constant. It can be seen that with this type of controller ω_e can equal zero at steady-state and V_m will still have a non-zero value, coming from the integral term. In fact, if ω_e deviates from zero by any amount, the value of the integral term will change in such a way as to correct the error. A controller of this type is known as a "PI" controller, or "proportional-integral". The time it takes to make $\omega_m = \omega_r$, or even whether the controller works at all, depends on the values chosen for K_p and K_I . The time delay for ω_m to approach a new ω_r is called the response time, and is critical in many applications including the scanner. Even greater control over response time can be achieved by feeding back the derivative of the error. Then the controller expression becomes:

$$V_m(t) = K_p \omega_e(t) + K_I \int_0^t \omega_e(\tau) d\tau + K_D \frac{d}{dt} \omega_e(t) \quad (2)$$

' K_D ' is the derivative control constant and this is known as full 'PID' control. This is a very versatile control method used in many applications requiring quick response and no

steady-state error.

In order to choose the proper values for the feedback gains K_P , K_I , and K_D it is first necessary to understand the dynamics of the system to be controlled. In this case that means knowing the characteristics of the particular DC motor being used, and the characteristics of the motor's load such as moment of inertia, viscous drag, etc. The system dynamics must be described by equations that comprise a mathematical model of the system. The model should be as close as possible to the real system but some error is permissible since a feedback-controller will correct for it. There are two different approaches to computing the feedback gains, once the model of the system is derived. They both center around classical control theory. In the algebraic approach the equations describing the controller are incorporated into the system model to give a complete closed-loop system equation. When the desired closed-loop behavior of the system has been decided on, the closed-loop equation can be manipulated and solved for the values of the feedback gains that will give such a response. This approach was the first one attempted for the DC motor, but was abandoned because the equations became too unwieldy. The second approach involves using a package of computer programs for manipulating linear systems. The package, called "LINSYS", was developed at the University of Illinois [8]. It requires that the system be described in matrix form. The desired behavior of the closed-loop system is specified by requesting values for the system's closed-loop poles.

LINSYS then computes the feedback gains that give the system this behavior. This approach has been used throughout the design of the DC motor controller.

CHAPTER V

MODEL OF ARMATURE-CONTROLLED DC MOTOR

The most popular DC servomotors use armature control and have permanent-magnet field poles. Because of its relatively low cost and linear characteristics, this type of motor was selected for use in the scanner. It is controlled by varying the voltage applied to the terminals of its rotating armature^[9].

An electro-mechanical model of such a motor is shown in Figure 7. Summing the voltages around the loop gives

$$V_m = L_a \frac{di}{dt} + Ri + K_v \omega_m \quad (3)$$

The torque is described by

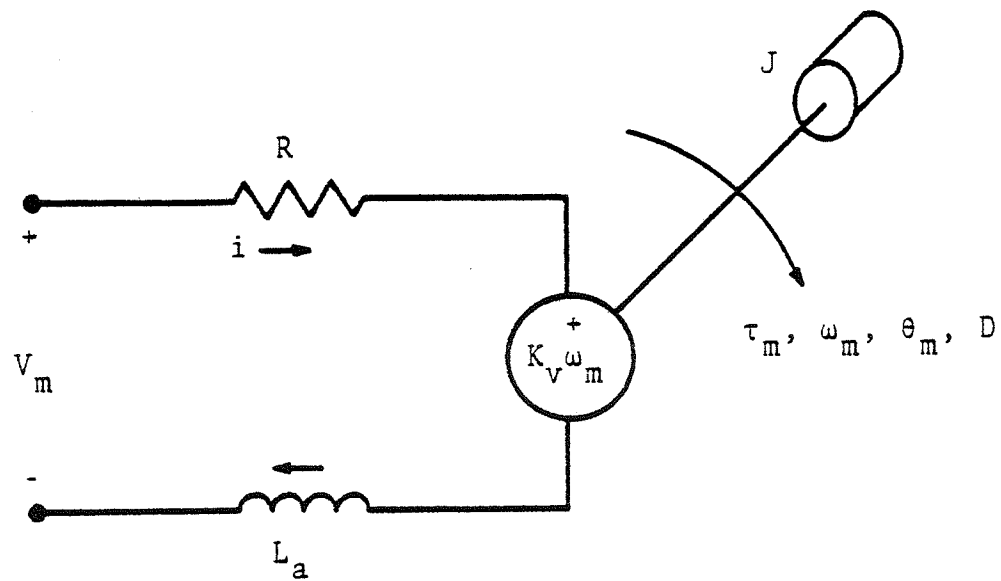
$$\tau_m = K_\tau i + D\omega_m \quad (4)$$

and the angular acceleration is

$$\frac{d\omega_m}{dt} = \frac{1}{J} \tau_m \quad (5)$$

These can easily be manipulated into separate electrical and mechanical equations.

$$\text{electrical: } \frac{di}{dt} = -\frac{R}{L_a} i - \frac{K_v}{L_a} \omega_m + \frac{1}{L_a} V_m \quad (6)$$



- τ_m - Torque on motor shaft
- ω_m - Angular velocity of shaft
- θ_m - Angular position of shaft
- D - Viscous damping factor
- J - Moment-of-inertia of system
- K_v - Armature back-emf constant
- R - Armature resistance
- L_a - Armature inductance
- V_m - Armature voltage
- i - Armature current

Figure 7. DC Motor Model.

$$\text{mechanical: } \frac{d\omega_m}{dt} = \frac{K_\tau}{J} i + \frac{D}{J} \omega_m \quad (7)$$

Of primary interest in the design of a servo control system is the relationship between the applied voltage V_m and the angular velocity ω_m . The simplest way to find this is through the Laplace transform technique. The transform of equation (6) is

$$sI(s) - i(0) = -\frac{R}{L_a} I(s) - \frac{K_V}{L_a} \Omega_m(s) + \frac{1}{L_a} V_m(s) \quad (8)$$

and (7) transforms to

$$s\Omega_m(s) - \omega_m(0) = \frac{K_\tau}{J} I(s) + \frac{D}{J} \Omega_m(s) \quad (9)$$

Now it is possible to manipulate (8) and (9) algebraically to find the transfer function $\frac{\Omega_m(s)}{V_m(s)}$, after letting the initial conditions equal zero.

$$\frac{\Omega_m(s)}{V_m(s)} = \frac{K_\tau}{(L_a s + R)(Js - D) + K_\tau K_V} = \frac{K_\tau}{JL_a \left(s + \frac{R}{L_a}\right) \left(s - \frac{D}{J}\right) + K_\tau K_V} \quad (10)$$

If the time-domain behavior of the motor is desired for any given voltage waveform $V_m(t)$, the transformed voltage expression, $V_m(s)$, can be substituted in (10), giving an expression for $\Omega_m(s)$ in the frequency domain. This expression can be converted back to the time domain by taking its inverse Laplace

transform, giving $\omega_m(t)$ for the given $V_m(t)$. This is a time-consuming process and won't be illustrated here.

It is often desired to know the steady-state velocity of a DC motor with constant $V_m(t)$. If $V_m(t)$ is constant the steady-state velocity is found through the Final-Value Theorem. It states that if $F(s) = L\{f(t)\}$, then

$$\lim_{t \rightarrow \infty} f(t) = \lim_{s \rightarrow 0} sF(s) \quad (11)$$

Let $V_m(t) = v_m = \text{const.}$ Then $V_m(s) = L\{V_m(t)\} = \frac{v_m}{s}$. Using (11)

$$\begin{aligned} \lim_{t \rightarrow \infty} \omega_m(t) &= \lim_{s \rightarrow 0} s\Omega_m(s) \\ &= \lim_{s \rightarrow 0} s \frac{K_\tau}{JL_a \left(s + \frac{R}{L_a}\right) \left(s - \frac{D}{J}\right) + K_\tau K_V} \frac{v_m}{s} \end{aligned}$$

giving

$$\omega_{m,ss} = \frac{K_\tau}{K_\tau K_V - RD} v_m \quad (12)$$

According to (12), if a DC motor obeys the linear model in Figure 7, its steady-state velocity will be directly proportional to its applied voltage.

The aforementioned transfer function is used as the basis for algebraically determining the feedback values. In order to use the LINSYS package to compute the feedback, the system

must be described in matrix form,

$$\dot{x}(t) = Ax(t) + Bu(t) \quad (13)$$

$$y(t) = Cx(t) \quad (14)$$

where $x(t)$ is the system state vector, and $u(t)$ is the input to the system. In this case, $x = \begin{bmatrix} i \\ \omega_m \end{bmatrix}$ and $u = V_m$. The system output is $y(t)$, which represents the state-variables of the system that are available for measurement. The electric and mechanical equations, (6) and (7), are used to find the values for A and B, giving

$$\frac{d}{dt} \begin{bmatrix} i \\ \omega_m \end{bmatrix} = \begin{bmatrix} -R/L_a & -K_v/L_a \\ K_t/J & D/J \end{bmatrix} \begin{bmatrix} i \\ \omega_m \end{bmatrix} + \begin{bmatrix} 1/L_a \\ 0 \end{bmatrix} V_m \quad (15)$$

where

$$A = \begin{bmatrix} -R/L_a & -K_v/L_a \\ K_t/J & D/J \end{bmatrix} \text{ and } B = \begin{bmatrix} 1/L_a \\ 0 \end{bmatrix}$$

"C" is the output matrix and will be defined later. This method of defining the system is known as the matrix state equation.

The specifications and parameter values for a typical DC servomotor used in the scanner are in Appendix C.

CHAPTER VI

ANALYSIS AND DESIGN OF A VELOCITY CONTROL SYSTEM

As was stated earlier, the simplest type of velocity control uses a proportional controller, with $V = K_P(\omega_r - \omega_m)$. This controller has the drawback of permitting a steady-state error to exist in the motor's velocity. With a full PID controller the steady-state error will be zero. This can be seen by describing the closed-loop system of the motor and PID controller, shown in Figure 5. Let the PID controller be described in the frequency domain by

$$C_V(s) = \frac{V_m(s)}{\Omega_e(s)} = K_P + K_I \frac{1}{s} + K_D s \quad (16)$$

The transfer function of the motor is

$$M(s) = \frac{\Omega_m(s)}{V_m(s)} = \frac{K_\tau}{JL_a(s + \frac{R}{L_a})(s - \frac{D}{J}) + K_\tau K_V} \quad (17)$$

To examine the steady-state error in ω_m it is necessary to find the transfer function of the closed-loop system,

$$\frac{\Omega_m(s)}{\Omega_r(s)} = \frac{C_V(s)M(s)}{1 + C_V(s)M(s)} \quad (18)$$

which becomes

$$\frac{\Omega_m(s)}{\Omega_r(s)} = \frac{K_\tau K_D s^2 + K_\tau K_P s + K_\tau K_I}{JL_a s^3 + (RJ - DL_a + K_\tau K_D) s^2 + (K_\tau K_V + K_\tau K_P - DR) s + K_\tau K_I} \quad (19)$$

To determine the steady-state behavior of ω_m , the reference velocity is made constant and the Final-Value Theorem (11) is applied.

$$\Omega_r(s) = \frac{\omega_r}{s} \quad (20)$$

$$\omega_{m,ss} = \lim_{s \rightarrow 0} s \frac{K_\tau K_D s^2 + K_\tau K_P s + K_\tau K_I}{JL_a s^3 + (RJ - DL_a + K_\tau K_D) s^2 + (K_\tau K_V + K_\tau K_P - DR) s + K_\tau K_I} \frac{\omega_r}{s} \quad (21)$$

To examine the case for non-integral control, K_I is set to zero, and $\omega_{m,ss}$ becomes

$$\omega_{m,ss} = \frac{K_\tau K_P}{K_\tau K_V + K_\tau K_P - DR} \omega_r \quad (22)$$

From this, the steady-state error can be written as

$$e_{ss} = \omega_r - \omega_{m,ss} = \left(1 - \frac{K_\tau K_P}{K_\tau K_V + K_\tau K_P - DR}\right) \omega_r \quad (23)$$

It can be seen that the error actually increases with the requested velocity. The error decreases as $\frac{K_\tau K_P}{K_\tau K_V + K_\tau K_P - DR} \rightarrow 1$, which occurs when $K_P \rightarrow \infty$. A non-integral controller can be built that will have a small e_{ss} if a large feedback value is

used. The trouble with using a large feedback is that it makes the system sensitive to random disturbances, such as noise.

The alternative to a proportional controller with large gain is an integral controller. From equation (21) with $K_I \neq 0$ it is seen that for integral control, $\omega_{m,ss} = \omega_r$ and $e_{ss} = 0$. Integral control was chosen for the scanner's motors for this reason. Had simple proportional control been used, the high gain necessary for small e_{ss} may have introduced enough noise to take away the inherent smoothness of a DC motor.

Placing the closed-loop system poles by hand involves equating the desired characteristic equation (C.E.) to the C.E. of the closed-loop system, then solving for the feedback gains. For reasons of flexibility and simplicity, it was decided to rework the system into matrix form and place the poles using LINSYS.

LINSYS requires the system to be in the form of equations (13)-(15). The system and desired poles are then input to LINSYS and it returns a feedback matrix $F = [f_1 \ f_2 \ \dots \ f_n]$ where n is the number of system state-variables. The closed-loop system will have the requested eigenvalues (poles) if

$$\begin{aligned} u &= Fx \\ &= f_1x_1 + f_2x_2 + \dots + f_nx_n \end{aligned} \quad (24)$$

This is called full-state feedback. Nowhere does LINSYS require a reference input, such as ω_r , to place the poles. The

feedback is designed to bring the system to equilibrium (all derivatives zero) with the requested response pattern. Thus, during pole-placement, the reference input is considered zero. In a tracking problem such as velocity control, the actual reference is introduced in the feedback. A simple example of this involving non-integral control makes use of the system in equation (15). After specifying the system (A,B) and the required closed-loop poles to LINSYS, it will compute a matrix $F = [f_1 \ f_2]$. If the feedback is provided as in equation (24), then the system will track a velocity of zero. If feedback is provided in the form

$$u = f_1 x_1 + f_2 (x_2 - r) \quad (25)$$

equivalent to
$$V_m = f_1 i + f_2 (\omega_m - \omega_r) \quad (26)$$

then the system will adjust itself to minimize $(\omega_m - \omega_r)$ and the motor's velocity will be close to ω_r . Since this example does not provide integral control, there will be a steady-state error in tracking ω_r .

The full-state feedback that LINSYS provides may appear quite different in form than the controller expression in (2). They are, in fact, different representations of the same thing. It is easy to see how the f_2 term in (25) is equivalent to the K_p term in (2) since $\omega_e = \omega_r - \omega_m$ in (2). The f_1 term in (25) comes in place of the K_D term in (2) because $\frac{d}{dt} \omega_e = \frac{d}{dt} (\omega_r - \omega_m) = -\dot{\omega}_m$ since ω_r is constant. From (7) it is seen that $\dot{\omega}_m$

can be expressed in terms of i and ω_m , so feeding back $-\dot{\omega}_m$ with gain K_D in (2) is equivalent to feeding back i with gain f_1 in (26). The system being controlled in (25)-(26) has no state equivalent to the K_I term in (2) so full state feedback in this case will not provide integral control.

In order to use LINSYS to design an integral controller it is necessary to augment the system in (15) with a third state-variable to represent the integral of $\omega_m - \omega_r$. Then (15) becomes

$$\frac{d}{dt} \begin{bmatrix} i \\ \omega_m \\ \theta_d \end{bmatrix} = \begin{bmatrix} -R/L_a & -K_v/L_a & 0 \\ K_\tau/J & D/J & 0 \\ 0 & 1 & 0 \end{bmatrix} \begin{bmatrix} i \\ \omega_m \\ \theta_d \end{bmatrix} + \begin{bmatrix} 1/L_a \\ 0 \\ 0 \end{bmatrix} V_m + \begin{bmatrix} 0 \\ 0 \\ -\omega_r \end{bmatrix} \quad (27)$$

The new state is

$$\frac{d}{dt} \theta_d = \omega_m - \omega_r \quad (28)$$

or

$$\theta_d = \int_0^t (\omega_m - \omega_r) d\tau \quad (29)$$

The final term in (27) is the disturbance input. This term is omitted for purposes of pole placement. LINSYS will compute the values for $F = [f_1 \ f_2 \ f_3]$ so that with

$$\begin{aligned} V_m &= F_x \\ &= f_1 x_1 + f_2 x_2 + f_3 x_3 \end{aligned} \quad (30)$$

the system will go to equilibrium from any initial state with the requested response time. To implement this integral controller it is necessary to build an integrator for $(\omega_m - \omega_r)$. Then the third term in (30) becomes

$$f_3 x_3 = f_3 \int_0^t (\omega_m - \omega_r) d\tau \quad (31)$$

and it is easily seen to be equivalent to the K_I term in (2). Full state feedback for the augmented system in (27) is equivalent to full PID control.

A prerequisite to being able to build the integrator for the K_I term is the ability to measure ω_m . This would normally be done by means of a tachometer-generator connected to the motor shaft. Many servomotors have built-in tachometers, including the ones used for the scanner. The tachometer works quite well at producing a voltage proportional to velocity over most of the motor's operating range, but at low velocity the accuracy diminishes greatly. Much of the operation of the scanner will require low motor velocities, especially during positioning. For this reason an alternative had to be found to the direct tachometer approach.

In order to have feedback for the positioning operation, an optical shaft encoder is connected to the final driven shaft. This device produces an output pulse every time its shaft moves through a small angle (Appendix A). This device is also used in place of a tachometer for velocity control. This is done

by breaking up the integral term as shown

$$\int_0^t (\omega_m - \omega_r) d\tau = \int_0^t \omega_m d\tau - \int_0^t \omega_r d\tau \quad (32)$$

The first term on the right in (32) is simply the motor angle, θ_m , which can be measured very accurately by keeping a count of pulses from the encoder. The second term can be thought of as representing a "lead angle", θ_f , which increases at the rate desired of the motor's angle. The integral term can then be written to look like

$$f_3 x_3 = f_3 (\theta_m - \theta_f) \quad (33)$$

Whenever θ_m is unequal to θ_f the integral term contributes to the control voltage V_m in such a way as to minimize the difference.

As is seen, the integral velocity controller will try to cause θ_m to increase until it is equal to θ_f . This is equivalent to position control, where θ_f is the angular position being sought. In the case of velocity control, θ_f will be constantly increasing in the direction of ω_r . If the motor's velocity is less than ω_r , the difference angle $\theta_d = \theta_m - \theta_f$ will increase in magnitude, producing a larger contribution to V_m , which in turn will "close the gap". If ω_m gets too large θ_d will decrease in magnitude in turn slowing down the motor. How near θ_m is to θ_f is determined by the motor's voltage

requirement for maintaining the requested speed. If ω_r or the load on the motor is changed, θ_d will settle to a new equilibrium value that provides the needed voltage.

If this controller were to be used to control position ω_r would be set to zero and θ_f set to θ_r , the position sought. With $\omega_r = 0$, θ_f will remain constant. As long as θ_m does not equal θ_f a control voltage will be produced to close the gap. There is a drawback to this type of position control. Due to static friction, it is impossible to achieve zero error on positioning, similar to how non-integral velocity control left a steady-state error in velocity, as seen in (22) and (23). The steady-state position error can be decreased by using a large value for f_3 but this is dangerous because 3rd-order systems tend to become unstable when this is done. Whereas this controller provides integral control of velocity, it can be used to produce only non-integral control of position. A position controller that has no error would require still another feedback proportional to $\int(\theta_m - \theta_r)d\tau$, and the system would be 4th-order.

CHAPTER VII

STATE FEEDBACK WITH FULL-ORDER OBSERVER

Implementing an integral controller with full-state feedback requires knowing the current values of all state-variables, i , ω_m , and θ_m . Unless a tachometer is used to measure ω_m , the only state-variable that is directly measureable here is θ_m . If the system (A,C) is observable it is possible to design an observer that will predict the values of the other state-variables by measuring θ_m . "A" is the system matrix from (27)

$$A = \begin{bmatrix} -R/L_a & -K_v/L_a & 0 \\ K_\tau/J & D/J & 0 \\ 0 & 1 & 0 \end{bmatrix} \quad (34)$$

and "C" is the output matrix defining the system's output, or directly measureable state-variables. The output, y , is defined by

$$\begin{aligned} y &= Cx \\ &= [0 \quad 0 \quad 1] \begin{bmatrix} x_1 \\ x_2 \\ x_3 \end{bmatrix} \\ &= \theta_m \end{aligned} \quad (35)$$

since motor position is all that can be measured directly and this does not yet include θ_f (33).

An observer works by simulating the behavior of the system and correcting for any deviation between the real system and the observer's system. The observer's state is available and is used for feedback instead of the real system's state. The observer's state is denoted by \hat{x} , and ideally it will converge to x and remain there. The observer equation is

$$\frac{d}{dt} \hat{x} = A\hat{x} + Bu + K(y - \hat{y}) \quad (36)$$

$$\hat{y} = C\hat{x} \quad (37)$$

where A , B , and C are the same as for the real system. Since the observer will often start with initial conditions different from the system it's observing, the observer's state will typically be different from that of the system. This can also happen if (A,B) is a less-than-perfect model of the system. The 3rd term in (36) is to correct any error in the observed state. If the output from the observer, $C\hat{x}$, is not equal to the measured system output there is an error in the observer state. The matrix K provides a correction to the observer state based on the amount of this error, and is the "observer feedback matrix".

Determining a value for K is done in a way similar to how F was found to place the poles of (A,B) . If (36) is subtracted from the system equation,

$$\frac{d}{dt} x = Ax + Bu \quad (38)$$

the result is

$$\begin{aligned} \frac{d}{dt} (x - \hat{x}) &= A(x - \hat{x}) - K(Cx - C\hat{x}) \\ &= (A - KC)(x - \hat{x}) \end{aligned} \quad (39)$$

It is desired that $\hat{x} \rightarrow x$, or $(x - \hat{x}) \rightarrow 0$. If (A,C) is observable, K can be found so that $(x - \hat{x}) \rightarrow 0$ as rapidly as desired. This is equivalent to using K to place the poles of (A,C) the way F was used to place the poles of (A,B) in (30). LINSYS can be used to compute the value of K , given the desired observer poles.

This is called a full-order observer because it reconstructs the complete state of the system. It has the drawback of also reconstructing the measured state-variable, which is redundant. Nevertheless, a full-order observer is the simplest type to design. It is also possible to design a reduced order observer that observes only those state-variables that are not available through y . When state feedback is provided from the observer's state the system will have the same closed loop eigenvalues as if actual state feedback were provided, if the observer poles are faster (farther to the left) than the system's. Otherwise \hat{x} will not be able to track x and the system may be unstable. The poles of $(A - KC)$ should be chosen to be to the left of the

poles of $(A + BF)$ in the s -plane.

Ideally it may seem desirable to make the system and observer infinitely fast so $\hat{x} \rightarrow x$ and $\omega_m \rightarrow \omega_r$ immediately. A faster system requires larger feedback values, and there is a practical limit to how great a feedback can be used. Also, a slower system is more insensitive to noise. Noise in this case is any high frequency disturbance, or other inaccuracy in the system. If the system has a faster response it has a higher bandwidth and will attempt to track the noise, producing vibration and unsteadiness at the output. This would defeat the purpose of using a DC motor instead of a stepping motor as described earlier. If the observer has too fast a response it may tend to overcompensate for any inaccuracy in \hat{x} and the trajectory of \hat{x} will swing back and forth as it follows the trajectory of x , unless the implementation of the observer has high accuracy and low noise.

CHAPTER VIII

DISCRETE IMPLEMENTATION OF VELOCITY CONTROL

The preceding discussion centered on the design of a PID velocity controller, taking note of the requirements of the ultrasonic scanner. The controller is to be implemented on a microprocessor, which makes it a discrete controller. That is, it receives information about the system only at discrete time intervals kT , $k = 0, 1, 2, \dots$. It can only update its control output when it receives new input about the system, and the control stays constant during each interval (Figure 8). If the sampling and updating frequency is high the system with a discrete controller will resemble one with a continuous, analog controller. If the feedback-gains for a continuous system are used in a discrete controller, the sampling rate would have to be high or the system may become unstable.

It is possible to design a discrete controller with feedback gains "custom tailored" for a given sampling frequency. To do this it is necessary to know how much the system will change if its input is held constant for time T . Since a DC motor is a linear system it is possible to find the motor's state at time $t = (k + 1)T$ by summing its zero-input response and zero-state response over period T .

$$x[(k + 1)T] = \phi(T)x[kT] + \int_{t=0}^{t=T} \phi(t)Bdt u[kT] \quad (40)$$

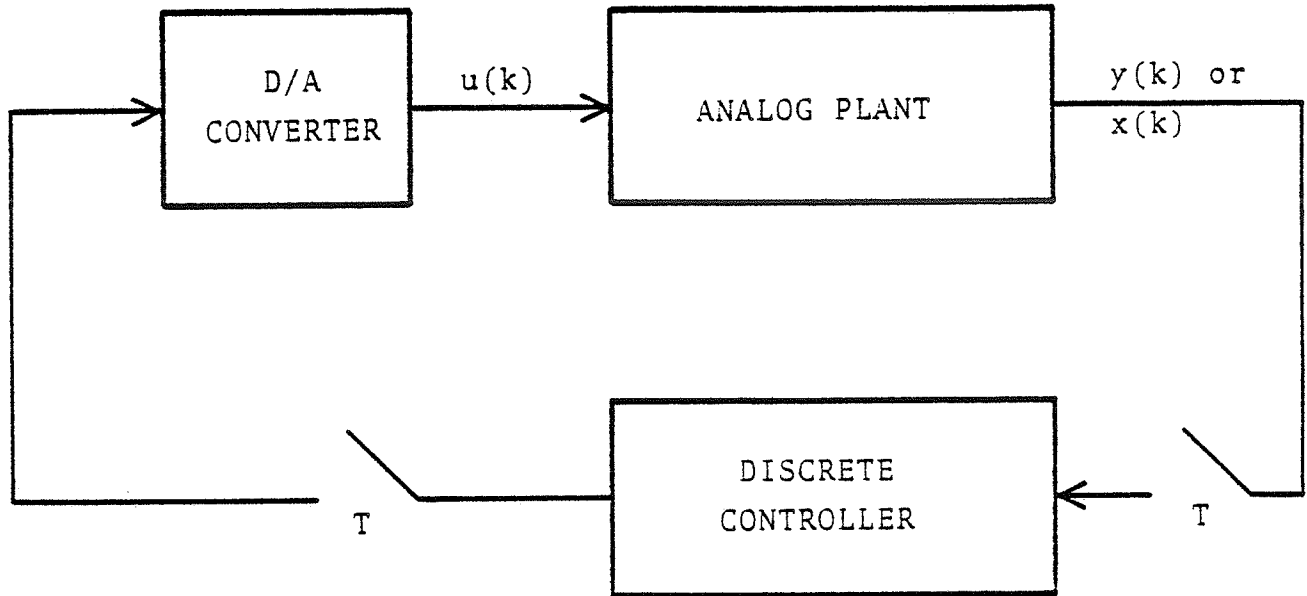


Figure 8. General Sampled-Data System.

The first term on the right in (40) is the zero-input response of the system, starting with its state at kT . The second term is the zero-state response for the control u that was last updated at $t = kT$. Since $u(kT)$ is a constant during the interval it was removed from within the integral. The matrix $\phi(t)$ is the state transition matrix, where

$$\phi(t) = L^{-1}\{(sI - A)^{-1}\} \quad (41)$$

A discrete state equation can be written from (40), analogous to the continuous state equation of (13) and (14). In this equation, $x(k)$ is written instead of $x(kT)$.

$$x(k + 1) = A_d x(k) + B_d u(k) \quad (42)$$

$$y(k) = C_d x(k) \quad (43)$$

The discrete system matrix is A_d ,

$$A_d = \phi(T) \quad (44)$$

and the discrete input matrix is B_d ,

$$B_d = \int_{t=0}^{t=T} \phi(t) B dt \quad (45)$$

In the output equation (43) the C_d matrix equals its continuous counterpart. Equation (42) is a difference equation, giving the state of the system one time period after a specific input was applied to it.

Using (40) it is possible to discretize the DC motor equations from (27). The final result is shown in (46)-(48). It should be noted that a system must be discretized for a particular T . If the period is changed, a new discretized system must be computed.

$$\begin{bmatrix} i(k+1) \\ \omega_m(k+1) \\ \theta_m(k+1) \end{bmatrix} = A_d \begin{bmatrix} i(k) \\ \omega_m(k) \\ \theta_m(k) \end{bmatrix} + B_d V_m(k) \quad (46)$$

See Appendix C for some values for matrixes A_d and B_d at various sampling periods T .

Determining the feedback to control a discrete system is basically the same as for a continuous system. It is desired to find a matrix or vector $F_d = [f_1 \ f_2 \ f_3]$ such that when

$$u(k) = F_d x(k) \quad (49)$$

the system states will go to zero after several iterations. The number of iterations it takes is determined by the discrete eigenvalues. If state variable x_j is uniquely associated with discrete eigenvalue z_j , then $x_j(k+1) = z_j x_j(k)$. If $|z_j| < 1$

$$\begin{aligned}
 & \left[\begin{array}{l} e^{\sigma T} \left[\cos \omega T + \frac{\sigma - D/J}{\omega} \sin \omega T \right] \\ e^{\sigma T} \left[\frac{K_T/J}{\omega} \sin \omega T \right] \\ \frac{K_V/J}{\sigma^2 + \omega^2} \left[e^{\sigma T} \left(\frac{\sigma}{\omega} \sin \omega T - \cos \omega T \right) + 1 \right] \\ \frac{K_V/J}{\sigma^2 + \omega^2} \left[e^{\sigma T} \left(\frac{\sigma}{\omega} \sin \omega T - \cos \omega T \right) + 1 \right] \\ \frac{e^{\sigma T}}{\sigma^2 + \omega^2} \left[\left(\omega + \frac{\sigma}{\omega} \right) \left(\sigma + \frac{R}{L_a} \right) \sin \omega T - \frac{R}{L_a} \cos \omega T \right] + \frac{R/L_a}{\sigma^2 + \omega^2} \\ e^{\sigma T} \left[\cos \omega T + \frac{\sigma + R/L_a}{\omega} \sin \omega T \right] \\ -e^{\sigma T} \frac{K_V/L_a}{\omega} \sin \omega T \end{array} \right] \\
 A_d = & \left[\begin{array}{l} 0 \\ 0 \\ 1 \end{array} \right]
 \end{aligned} \tag{47}$$

$$\begin{aligned}
 & \left[\begin{array}{l} \frac{1/L_a}{\sigma^2 + \omega^2} \left(e^{\sigma T} \left[\left(\omega + \frac{\sigma^2 - \sigma D/J}{\omega} \right) \sin \omega T + \frac{D}{J} \cos \omega T \right] - \frac{D}{J} \right) \\ \frac{K_V/J L_a}{\omega (\sigma^2 + \omega^2)} \left(e^{\sigma T} (\sigma \sin \omega T - \omega \cos \omega T) + \omega \right) \\ \frac{K_V/J L_a}{\sigma^2 + \omega^2} \left(\frac{e^{\sigma T}}{\sigma^2 + \omega^2} \left[\frac{\sigma^2 - \omega^2}{\omega} \sin \omega T - 2\sigma \cos \omega T \right] + \Gamma + \frac{2\sigma}{\sigma^2 + \omega^2} \right) \end{array} \right] \\
 B_d = & \tag{48}
 \end{aligned}$$

then x_j will go to zero and the closer z_j is to zero, the faster it will converge. If for all discrete eigenvalues z_i ,

$$|z_i| < 1 \quad (51)$$

the system is stable. The discrete eigenvalues are related to the continuous poles s_i by

$$z_i = e^{s_i T} \quad (52)$$

Computing the discrete feedback F_d is done in the same way as computing F in the continuous case, and can be done using LINSYS. The desired values for z_i are given to LINSYS along with A_d and B_d . LINSYS will compute F_d such that the poles of the closed-loop system,

$$\begin{aligned} x(k+1) &= A_d x(k) + B_d F_d x(k) \\ &= (A_d + B_d F_d) x(k) \end{aligned} \quad (53)$$

are at z_i . This value of F_d will only provide such a response if it is used at the sampling frequency for which A_d , B_d , and z_i were computed.

The process of determining the feedback for the scanner's controller starts with choosing s-plane poles that give the desired response for the continuous system. These poles are transformed to the z-plane using (52), after a suitable value for T is chosen. The matrices A_d and B_d must be computed for

the chosen T is and then they and the poles given to LINSYS. At this point LINSYS can compute F_d .

Since only one state-variable can be directly measured the others must be observed by a discrete observer. A discrete version of the observer of (36) must be designed and implemented on the microprocessor. For a stable system the poles of the observer must be chosen to lie to left of the system poles in the s -plane or closer to the origin in the z -plane. After choosing poles for the observer, LINSYS can compute the discrete observer feedback matrix K_d for the system matrix A_d and the output matrix $C_d = C$. The microprocessor must be programmed to implement the discrete version of (36), which is

$$\hat{x}(k + 1) = A_d \hat{x}(k) + B_d u(k) + K_d (y(k) - C_d \hat{x}(k)) \quad (54)$$

The system being observed is closed-loop and its input is computed from (49). This can be used to simplify (54) by substituting for $u(k)$.

$$\begin{aligned} \hat{x}(k + 1) &= A_d \hat{x}(k) + B_d F_d \hat{x}(k) - K_d C_d \hat{x}(k) + K_d y(k) \\ &= (A_d + B_d F_d - K_d C_d) \hat{x}(k) + K_d y(k) \end{aligned} \quad (55)$$

Equation (55) defines a discrete observer for a closed-loop system. At each iteration it computes a new value of \hat{x} based on the old value and the measured system output, y . The overall

discrete observer matrix is

$$A_{od} = A_d + B_d F_d - K_d C_d \quad (56)$$

Equation (55) must be modified slightly to incorporate the velocity setpoint. In the original augmented system of (27) \hat{x}_3 was not the true motor angle, but was the integral of $\omega_m - \omega_r$ (29). This must be taken into account in (55) where \hat{x}_3 represents the motor angle alone. The control expression is

$$\begin{aligned} u(k) &= V_m = F_d \hat{x}(k) \\ &= f_1 \hat{x}_1(k) + f_2 \hat{x}_2(k) + f_3 \hat{x}_3(k) \end{aligned} \quad (57)$$

As shown in (32) and (33), the third state-variable is the difference between θ_m and θ_f . For velocity control θ_f increases at the rate $T\omega_r$ each time period, since $\theta_f = \int_0^t \omega_r dt$. One way to modify (55) so that \hat{x}_3 becomes $\theta_m - \theta_f$ is to subtract $T\omega_r$ from \hat{x}_3 at each iteration. It is also necessary to modify the system output y . In (55) $y = \theta_m$, the measured motor angle. Since \hat{x}_3 was modified to become $\theta_m - \theta_f$ it is necessary to let

$$y(k) = \theta_m(k) - \theta_f(k) \quad (58)$$

This adjusts the observer's input, the system's "output", to be consistent with \hat{x}_3 . A new value of θ_f must be computed during

each control iteration.

A summary of the equations to be carried out by the micro-processor during each control cycle follows.

$$V_m = u(k) = F_d \hat{x}(k) \quad (59)$$

$$\hat{x}(k + 1) = A_{od} \hat{x}(k) - \begin{bmatrix} 0 \\ 0 \\ T\omega_r \end{bmatrix} + K_d(\theta_m(k) - \theta_f(k)) \quad (60)$$

$$\theta_f(k + 1) = \theta_f(k) + T\omega_r \quad (61)$$

The only quantity that is sensed from the outside world is $\theta_m(k)$, which is a count of pulses from the position encoder.

So as not to count unreasonably high, the counter for the encoder resets to zero after counting through 360° . If the encoder turns past zero in the negative direction, the count is set to the maximum. In this way each position has a unique angle associated with it. Whenever the encoder crosses zero the value of θ_f must be corrected so that the difference $\theta_m - \theta_f$ remains constant. The encoder has a zero-reference output line. This line is used to interrupt the processor each time the encoder crosses zero so that θ_f may be corrected.

Figure 9 is a simplified flowchart of the discrete controller-observer. Graphs of this controller's performance are found in Appendix D.

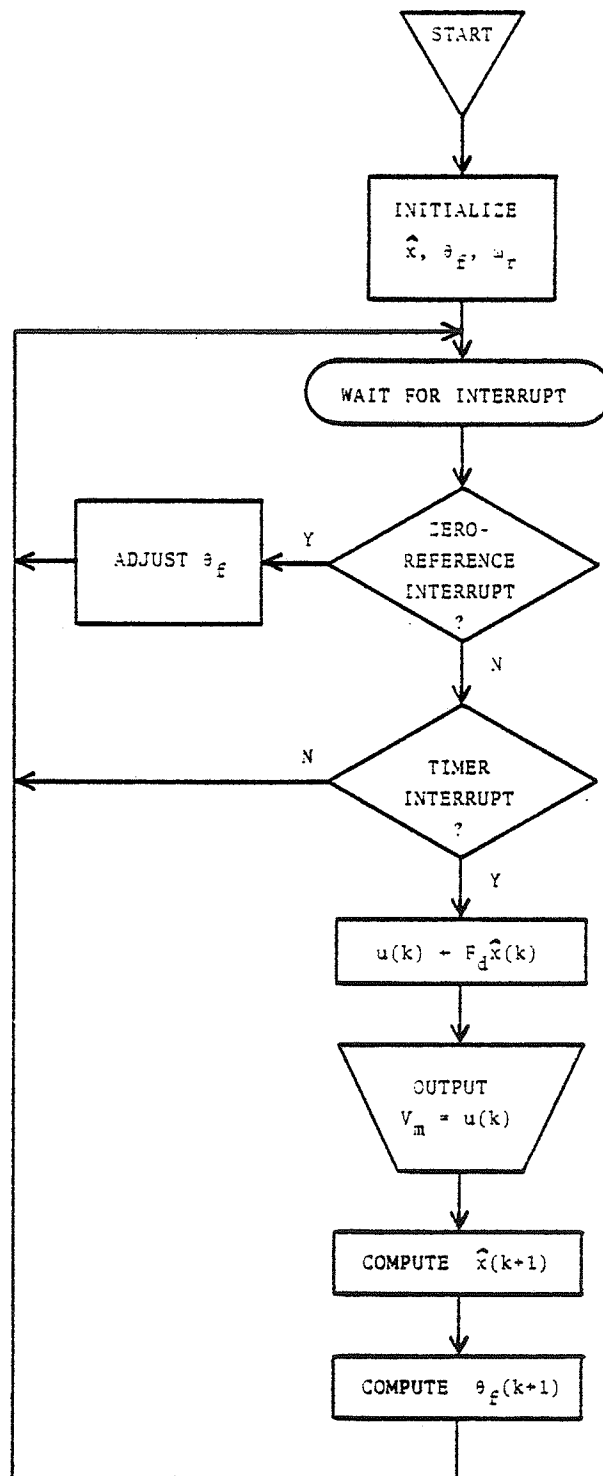


Figure 9. Velocity-Control Algorithm with Observer.

CHAPTER IXPOSITIONAL CONTROL

It has been explained that the velocity control system just described can be used to control motor position, but there will usually be a positioning error due to static friction. In a proportional position controller such as this one, the motor voltage is proportional to the positional error

$$V_m = C_p(\theta_r - \theta_m) \quad (62)$$

When the error becomes small enough that the voltage no longer overcomes static friction the motor stops, leaving a positioning error.

This error can be overcome by using the previously-designed integral velocity controller as the inner loop of the position controller shown in Figure 6. As long as there is a positional error, a nonzero velocity will be requested from the velocity controller to correct the error. However small the requested velocity is, the velocity controller will be able to overcome friction and move toward the requested position, since it uses integral control. Once the velocity controller has been designed the only parameter of position control that remains to be adjusted is C_p , the positional feedback constant, where

$$\omega_r = C_p(\theta_r - \theta_m) \quad (63)$$

The system is not in a form in which LINSYS can be used to find C_p . Rather than manipulate the new system into matrix form it was decided to modify the algorithm of (59)-(61) (Figure 9) to include (63). The modification is to compute a new ω_r at each iteration, rather than keep it fixed as in velocity control. When a zero-reference interrupt occurs, θ_r must be adjusted for the same reason θ_f had to be adjusted during velocity control. Figure 10 is a flowchart of the modified controller. With a controller that implements this algorithm it is possible to note the resultant system response for varying values of C_p , and determine the best value to use experimentally.

The experimental results were not too encouraging. For all but small values of C_p the system had a great deal of "ringing" and overshoot. When C_p was made small enough that this wouldn't happen, the system response was quite slow. Appendix D shows graphs of the new controller's performance for various values of C_p , using the same velocity controller as before. It can be seen that the system is severely underdamped for all but small C_p .

It may be possible to speed up the response and improve the damping by changing the poles of the velocity controller. A more direct approach is to redesign the position controller as a 4th-order system and use LINSYS to determine the feedback, the same way the velocity controller was designed. The result of this will be an integral position controller. The 3rd-order system (27) is augmented with a fourth state-variable, q , to

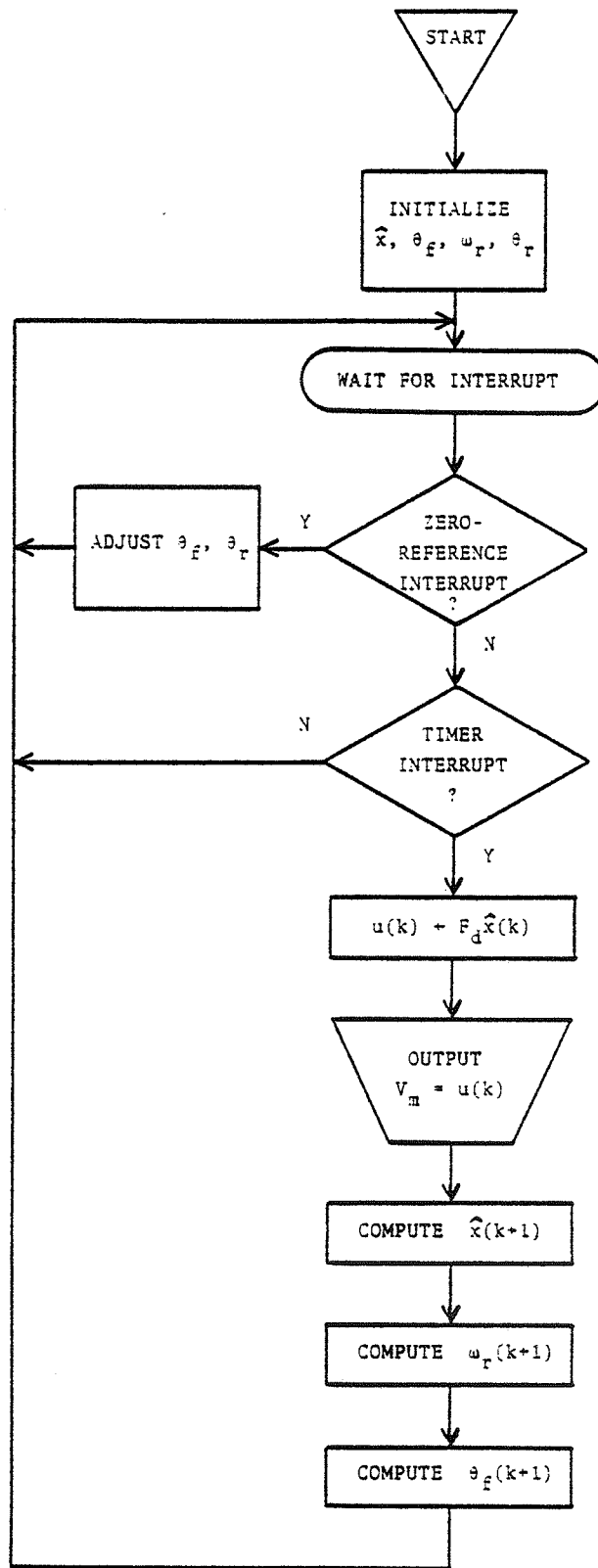


Figure 10. Simplified Position-Control Algorithm.

represent the integral of the position error,

$$q(t) = \int_0^t (\theta_m(\tau) - \theta_r(\tau)) d\tau \quad (64)$$

The augmented system becomes

$$\frac{d}{dt} \begin{bmatrix} i \\ \omega_m \\ \theta_m \\ q \end{bmatrix} = \begin{bmatrix} -R/L_a & -K_v/L_a & 0 & 0 \\ K_t/J & D/J & 0 & 0 \\ 0 & 1 & 0 & 0 \\ 0 & 0 & 1 & 0 \end{bmatrix} \begin{bmatrix} i \\ \omega_m \\ \theta_m \\ q \end{bmatrix} + \begin{bmatrix} 1/L_a \\ 0 \\ 0 \\ 0 \end{bmatrix} V_m + \begin{bmatrix} 0 \\ 0 \\ 0 \\ -\theta_r \end{bmatrix} \quad (65)$$

It should be noted that the third state-variable is θ_m and not θ_d as in (27). In (27) the third state-variable was the integral of the velocity error but in (65) the reference velocity is set to zero so the third state-variable is the motor position, θ_m . With full-state feedback, the control voltage becomes

$$V_m = f_1 i + f_2 \omega_m + f_3 \theta_m + f_4 \int_0^t (\theta_m - \theta_r) d\tau \quad (66)$$

If the motor is told to seek a position but stops in the wrong place because of friction, the fourth term in (66) will increase until V_m is great enough to overcome the friction.

When it is desired for the system in (65) to have a constant motor velocity, ω_r can be entered as a disturbance as shown in (67).

$$\frac{d}{dt} \begin{bmatrix} i \\ \omega_m \\ \theta_d \\ q \end{bmatrix} = \begin{bmatrix} -R/L_a & -K_v/L_a & 0 & 0 \\ K_\tau/J & D/J & 0 & 0 \\ 0 & 1 & 0 & 0 \\ 0 & 0 & 1 & 0 \end{bmatrix} \begin{bmatrix} i \\ \omega_m \\ \theta_d \\ q \end{bmatrix} + \begin{bmatrix} 1/L_a \\ 0 \\ 0 \\ 0 \end{bmatrix} V_m + \begin{bmatrix} 0 \\ 0 \\ -\omega_r \\ -\theta_r \end{bmatrix} \quad (67)$$

In this system the third state-variable is written as θ_d and has the same meaning as in (27), it being the difference angle between the motor position and the integral of ω_r . The control voltage from (67) is

$$V_m = f_1 i + f_2 \omega_m + f_3 \theta_d + f_4 \int_0^t (\theta_d - \theta_r) d\tau \quad (68)$$

If θ_r is any arbitrary constant, the closed-loop system of (67) and (68) will settle to equilibrium with $\theta_d = \theta_r$ and $\omega_m = \omega_r$.

Since this 4th-order system is completely controllable the feedback gains f_i can be chosen for any choice of closed-loop eigenvalues. This allows the positioning system to be designed for a fast response without excessive overshoot. The disadvantage to this approach is that 4th-order systems are less stable than 3rd-order, so fluctuations in system parameters are more likely to cast the system into instability. Furthermore, if the only state-variable available for measurement is θ_m it is necessary to build an observer to facilitate full-state feedback. If the observed state is "noisy", due to inaccuracies in the model or the observer being too sensitive, the system may become unstable.

It is undesirable to build a 4th-order observer for this system, since the 4th state-variable is an artificial one and observing it would be redundant. No other state-variable in the system depends on q , so the 3rd-order observer for the system in (34) and (35) can be used. This significantly reduces the amount of calculating that must be done during each iteration of the control algorithm.

Determining the discrete feedback gains and designing the discrete observer is the same as for velocity control, except that to compute the feedback the discrete form of the system in (65) is used. Since the observer is of a lower order than the augmented system, the simplification of the observer expression shown in (55) must be modified. One way this can be done is by letting

$$\begin{aligned}\hat{x}(k+1) &= A_d \hat{x}(k) + B_d u(k) - K_d C_d \hat{x}(k) + K_d y(k) \\ &= (A_d - K_d C_d) \hat{x}(k) + B_d u(k) + K_d y(k)\end{aligned}\tag{69}$$

In these expressions, A_d , B_d , K_d , and C_d are the previous matrices from the 3rd-order velocity-control system. The control $u(k)$ is computed with the 4th-order feedback gains,

$$u(k) = f_1 \hat{x}_1(k) + f_2 \hat{x}_2(k) + f_3 \hat{x}_3(k) + f_4 q(k)\tag{70}$$

The control algorithm is complete when the reference inputs for

velocity and position are included. It resembles the velocity controller in (59)-(61).

$$V_m = u(k) = [f_1 \ f_2 \ f_3 \ f_4] \begin{bmatrix} \hat{x}(k) \\ \text{----} \\ q(k) \end{bmatrix} \quad (71)$$

$$\hat{x}(k+1) = (A_d - K_d C_d) \hat{x}(k) - \begin{bmatrix} 0 \\ 0 \\ T\omega_r \end{bmatrix} + B_d u(k) + K_d (\theta_m(k) - \theta_f(k)) \quad (72)$$

$$q(k+1) = q(k) + T[\theta_m(k) - \theta_f(k) - \theta_r] \quad (73)$$

$$\theta_f(k+1) = \theta_f(k) + T\omega_r \quad (74)$$

Velocity control on the above system is achieved by setting ω_r to the desired velocity and θ_r to any constant, typically zero. Positioning is accomplished by setting ω_r and θ_f to zero and initializing \hat{x}_3 to θ_m . Then, when θ_r is set to the desired position, the motor will move there. Had θ_f not been set to zero, the motor would have turned to a position such that

$$\theta_m - \theta_f = \theta_r.$$

APPENDIX ASHAFT POSITION SENSING

The microprocessor controller is responsible for keeping track of the transducers' position angles, α , β , and γ , so that position information can be transmitted to the 7/32 computer while ultrasonic data is being taken. This information can also be used to determine the rate at which a given angle is changing. The task of position sensing is accomplished by connecting an optical shaft encoder to the drive shaft of each degree of freedom.

An encoder consists of a "slotted" disk mounted on a shaft. A beam of light is passed through the disk and is sensed by a photocell. As the shaft turns the light beam gets interrupted, causing the photocell to emit a voltage that varies with the motion of the disk. The photocell output gets passed to a conditioning circuit which processes it to standard logic voltages, and is then transferred out of the encoder. The encoders used in the scanner have three output lines, CCW, CW, and ZREF. If the encoder's shaft is being turned in a counter-clockwise direction the CCW line is pulsed at a rate of 10 pulses per degree of shaft rotation. The line is at ground potential otherwise. The same is true of the CW line for clockwise shaft rotation. There is a separate channel of information on the encoder's disk for zero-reference. The ZREF line is pulsed once for each rotation of the shaft as it moves

past a fixed point.

The motion of each transducer is induced by its respective DC motor through several reduction gears. This increases the effective torque and improves the positioning accuracy, but also introduces backlash into the system. So as to accurately know each transducer's position despite the backlash, each encoder is directly connected to the shaft on which its degree-of-freedom pivots. It is necessary to know the position of each transducer to within 0.1° , so encoders with 0.1° of accuracy were chosen.

A shaft's absolute position can be determined by counting pulses from the encoder (Figure A-1). A bidirectional binary counter is driven by the encoder outputs, the CCW line causing it to count up and the CW line causing it to count down. A counterclockwise shaft motion was chosen to be positive. The counter is never permitted to reach a value higher than 3599, since at 10 pulses per degree the encoder produces 3600 pulses per turn. The encoder's ZREF line will reset the counter to zero if it attempts to count higher than 3599 while turning counterclockwise. If the encoder is turned clockwise past zero the counter will automatically be loaded with 3599, and is never allowed to go negative. In this way each position of the encoder shaft has a unique angle associated with it. The counter associated with an encoder is the position register for that degree of freedom. It is connected to the microprocessor's bus and can be read by the control program. When the

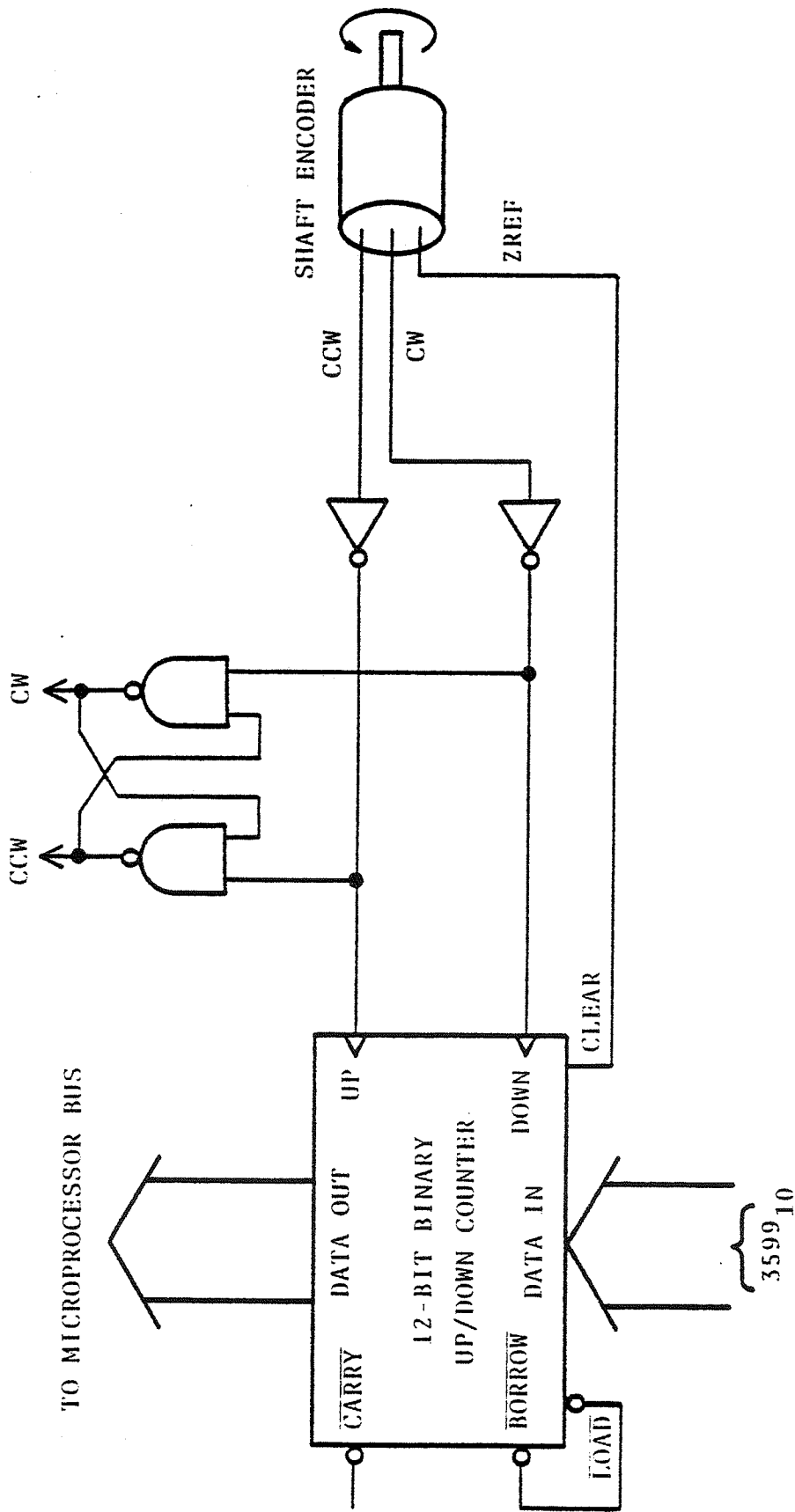


Figure A-1. Position Sensing.

system is powered-on initially the position register will not reflect the position of its associated transducer. This is dealt with by instructing each motor to move in a predetermined direction until the occurrence of a pulse from its ZREF line. This will automatically initialize its position register and inform the microprocessor controller that this transducer is at its "home" position. An R-S flipflop connected across the inputs to the counter keeps track of the most recent direction in which the shaft moved. This signal is also read by the microprocessor, and is used by parts of the control program.

APPENDIX BPULSED MOTOR CONTROL

The DC motors in the scanner are operated over a wide range of speeds, and under viscous loading conditions since the transducers are immersed in water. A significant amount of torque is required to rapidly accelerate the transducers to their required scanning speed and keep the speed constant. As seen in equations (4) and (7) the motor's torque is proportional to the current through its armature, and as the velocity through a viscous medium increases the current-requirements of the motor to counteract the drag increase. From equation (12) it is seen that the motor's steady-state speed is proportional to its supply voltage.

The microprocessor controller will output a control byte representing a motor voltage during each control cycle. Two approaches to powering the motor were considered: sending the byte to a digital to analog converter (DAC) and then to a power amplifier, or using the byte to control a pulsed voltage to the motor. Due to the wide range of voltages and currents that a single motor requires, pulsed voltage control was chosen. This is because a linear power amplifier will have to drop a significant voltage when operated below full power, which requires extensive heat sinking and raised questions of reliability.

The pulsing method that was chosen involves varying the duty cycle of a pulse stream that is of fixed frequency,

illustrated in Figure B-1. All pulses are of fixed height, and a higher effective voltage is equivalent to wider pulses. This pulse-width modulation method was chosen because it is straightforward to implement with digital circuitry. A question arose as to whether a DC motor would behave with a pulsed voltage similar to when it is given the equivalent continuous voltage. The DC-motor model of equations (6) and (7) was subjected to a computer simulation using IBM's Continuous Systems Modeling Program (CSMP III)^[10]. In the simulation, V_m was allowed to be both continuous and pulsed. As long as the pulse period was less than the motor's response time there was very little difference between the two cases. The steady-state velocity was the same in each case.

The circuit that receives the control byte is shown in simplified form in Figure B-2. A 1 MHz clock is continuously supplied to an 8-bit binary counter. This clock frequency is not critical, but was chosen because it could conveniently be tapped from the microprocessor. The counter's output is sent to an 8-bit magnitude-comparator circuit, to be compared to the control byte. As long as the control byte is greater than the value in the counter the comparator outputs a signal to turn on the motor. When the counter exceeds the value of the control byte the output pulse is turned off, and stays off until the counter resets itself to zero. A higher value of control byte will create longer pulses. The microcomputer outputs a ninth bit, separate from the voltage-byte, to determine motor

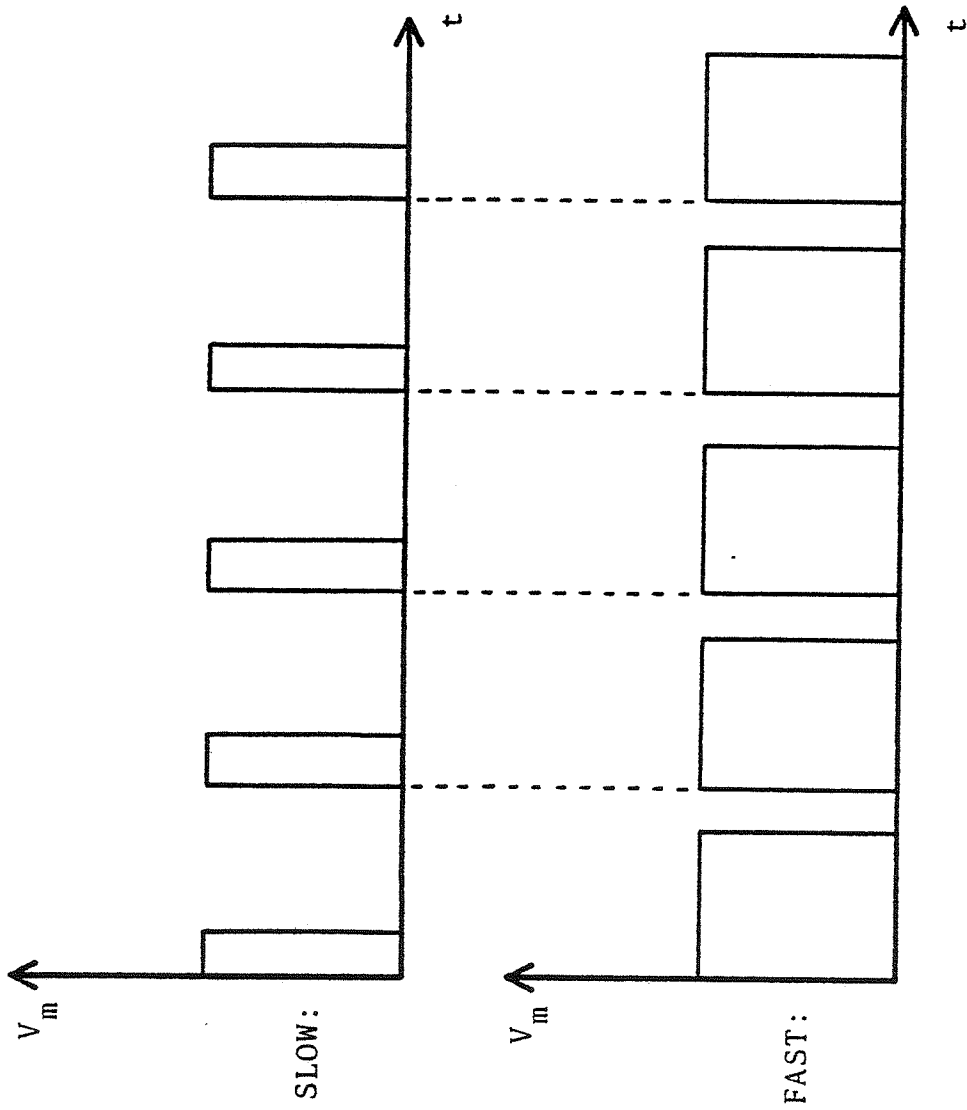


Figure B-1. Pulse-Width Modulation.

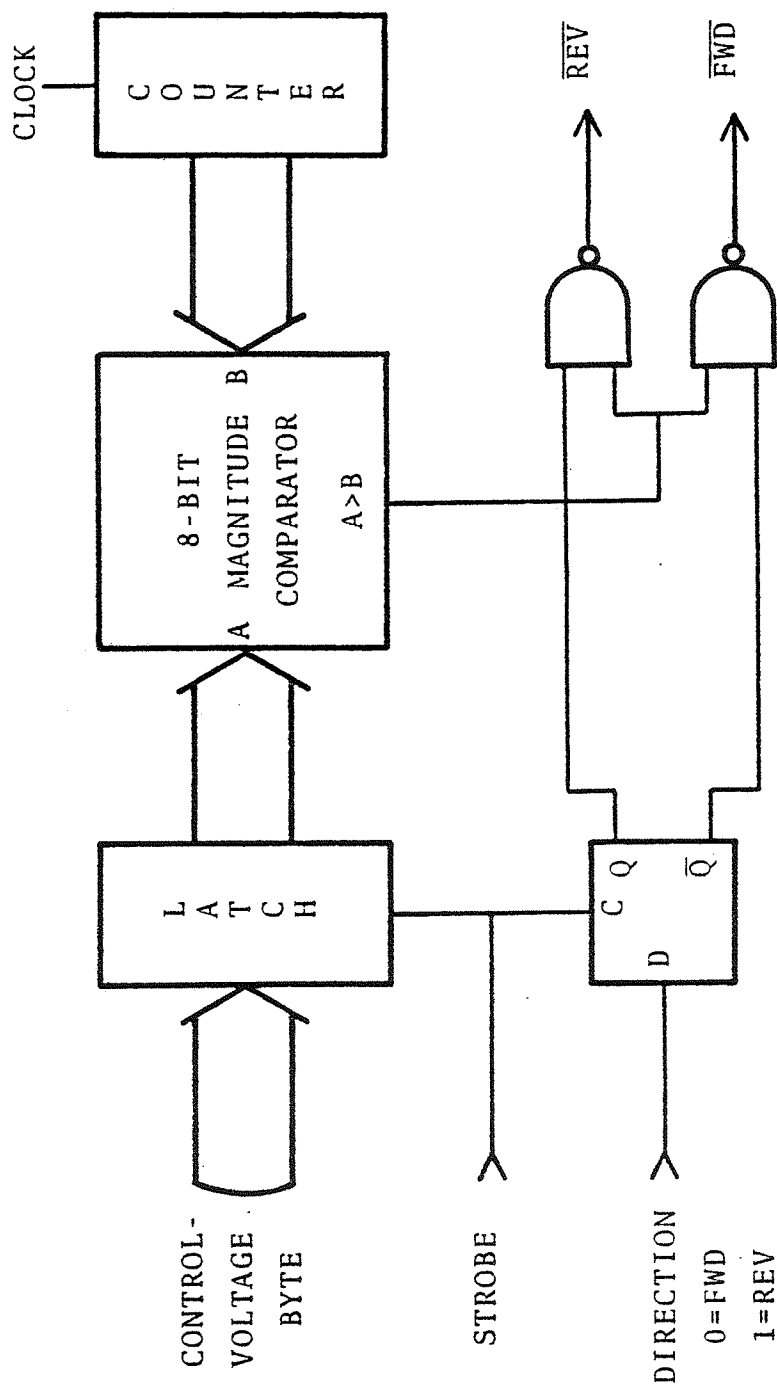


Figure B-2. Pulse-Width Generator.

direction. This bit routes the voltage pulses to the correct side of the bidirectional driver circuit.

The motor driver circuit is shown in Figure B-3. Power is applied to the motor by bringing either the $\overline{\text{FWD}}$ or $\overline{\text{REV}}$ input low. These lines are normally high. With the inputs high, Q_3 , Q_2 , Q_6 and Q_5 are all saturated, bringing the motor terminals close to ground. When $\overline{\text{FWD}}$ goes low, Q_3 and Q_2 stop conducting causing Q_1 to turn on. Current is driven through Q_1 and D_1 to the motor, and then through Q_5 to ground. The same is true when $\overline{\text{REV}}$ goes low and $\overline{\text{FWD}}$ is high. This circuit requires only a single power supply. Heat sinking is not required because the transistors are either on or off; they are never required to dissipate too much power.

A graph of the performance of this type of motor driver is shown in Figure B-4. The motor that was used is the one documented in Appendix C. Velocity measurements were made using the motor's built-in tachometer. It can be seen that the steady-state motor velocity is very linear with respect to the control byte. The graph does not go through the origin due to static friction.

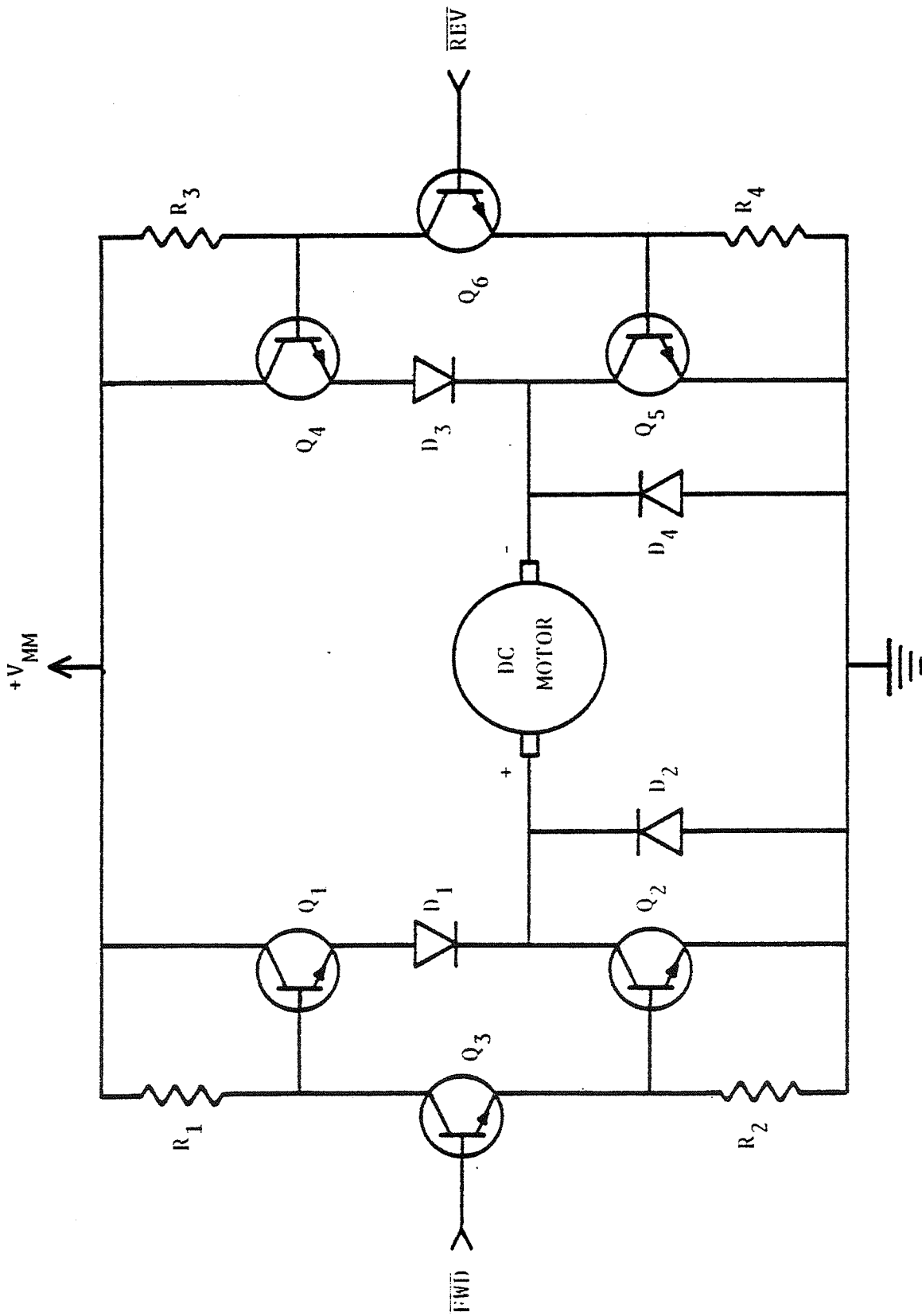


Figure B-3. Bidirectional Motor Driver.

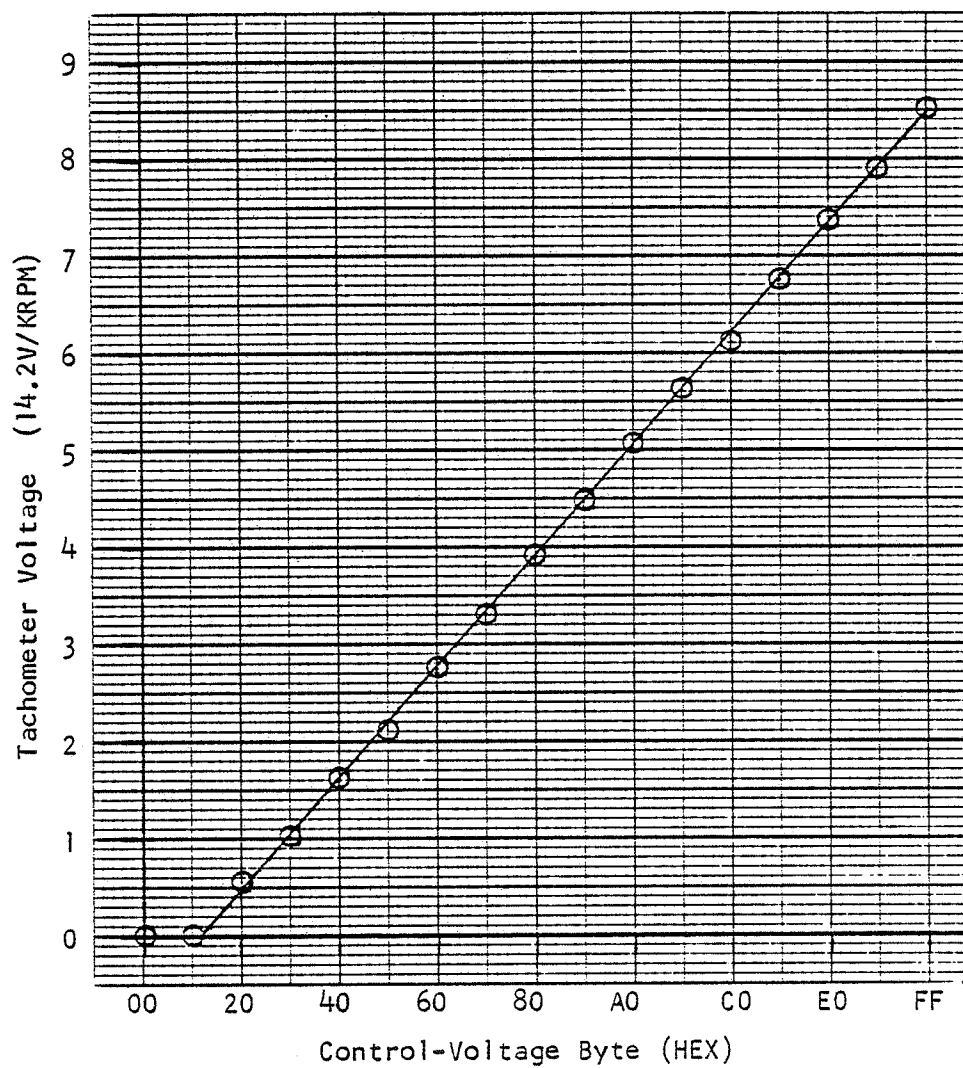


Figure B-4. Linearity of Pulsed Motor-Control.

APPENDIX CNUMERICAL CONSTANTS

Specifications for the Electro-Craft Model 0660-06-011 Permanent-Magnet DC Servomotor^[11]:

MOTOR

Torque Constant	K_T	21 oz-in/A	$\pm 10\%$
Voltage Constant	K_V	16 V/KRPM or 0.1528 V-sec/rad	$\pm 10\%$
Armature Resistance	R	1.15 Ω	@25°C $\pm 15\%$
Moment of Inertia	J	0.032 oz-in-sec ²	
Viscous Damping Factor	D	-1.0 oz-in/KRPM	
Static Friction Torque		7 oz-in	
Armature Inductance	L_a	4 mH	

BUILT-IN TACHOMETER

Voltage Gradient	K_T	14.2 V/KRPM	$\pm 10\%$
Terminal Resistance	R_T	750 Ω	@25°C $\pm 15\%$
Armature Inductance	L_T	140 mH	
Ripple Amplitude		5% of DC output	
Ripple Frequency		11 Cycles/Revolution	

Using these values, the motor-model of equation (27) becomes:

$$\frac{d}{dt} \begin{bmatrix} i \\ \omega_m \\ \theta_m \end{bmatrix} = \begin{bmatrix} -287.5 & -38.2 & 0 \\ 647.9 & -0.2946 & 0 \\ 0 & 1 & 0 \end{bmatrix} \begin{bmatrix} i \\ \omega_m \\ \theta_m \end{bmatrix} + \begin{bmatrix} 250 \\ 0 \\ 0 \end{bmatrix} V_m$$

The discrete version of this system is given in (46)-(48). The values of A_d and B_d for sampling rates of 10 Hz and 50 Hz are given here.

For $T = 0.1$ sec

$$A_d = \begin{bmatrix} 3.78 \times 10^{-7} & -4.76 \times 10^{-8} & 0 \\ 8.07 \times 10^{-7} & 7.36 \times 10^{-7} & 0 \\ 2.61 \times 10^{-2} & 1.16 \times 10^{-2} & 1 \end{bmatrix} \quad B_d = \begin{bmatrix} 2.966 \times 10^{-3} \\ 6.522 \\ 5.766 \times 10^{-1} \end{bmatrix}$$

For $T = 0.02$ sec

$$A_d = \begin{bmatrix} -1.048 \times 10^{-1} & -3.208 \times 10^{-2} & 0 \\ 5.441 \times 10^{-1} & 1.364 \times 10^{-1} & 0 \\ 2.252 \times 10^{-2} & 1.083 \times 10^{-2} & 1 \end{bmatrix} \quad B_d = \begin{bmatrix} 2.125 \times 10^{-1} \\ 5.630 \\ 5.972 \times 10^{-2} \end{bmatrix}$$

The units for these numbers are (-represents unitless):

$$[A_d] = \begin{bmatrix} - & \text{A-sec} & - \\ 1/\text{A-sec} & - & - \\ 1/\text{A} & \text{sec} & - \end{bmatrix} \quad [B_d] = \begin{bmatrix} \text{A/V} \\ \text{rad/V-sec} \\ \text{rad/V} \end{bmatrix}$$

The design of a typical system is now shown. Choose continuous-system poles: $s_i = -20, -40 \pm j40$. These poles were chosen because of the critically-damped response they produce. This was determined with a graphing package included in LINSYS (Figure C-1).

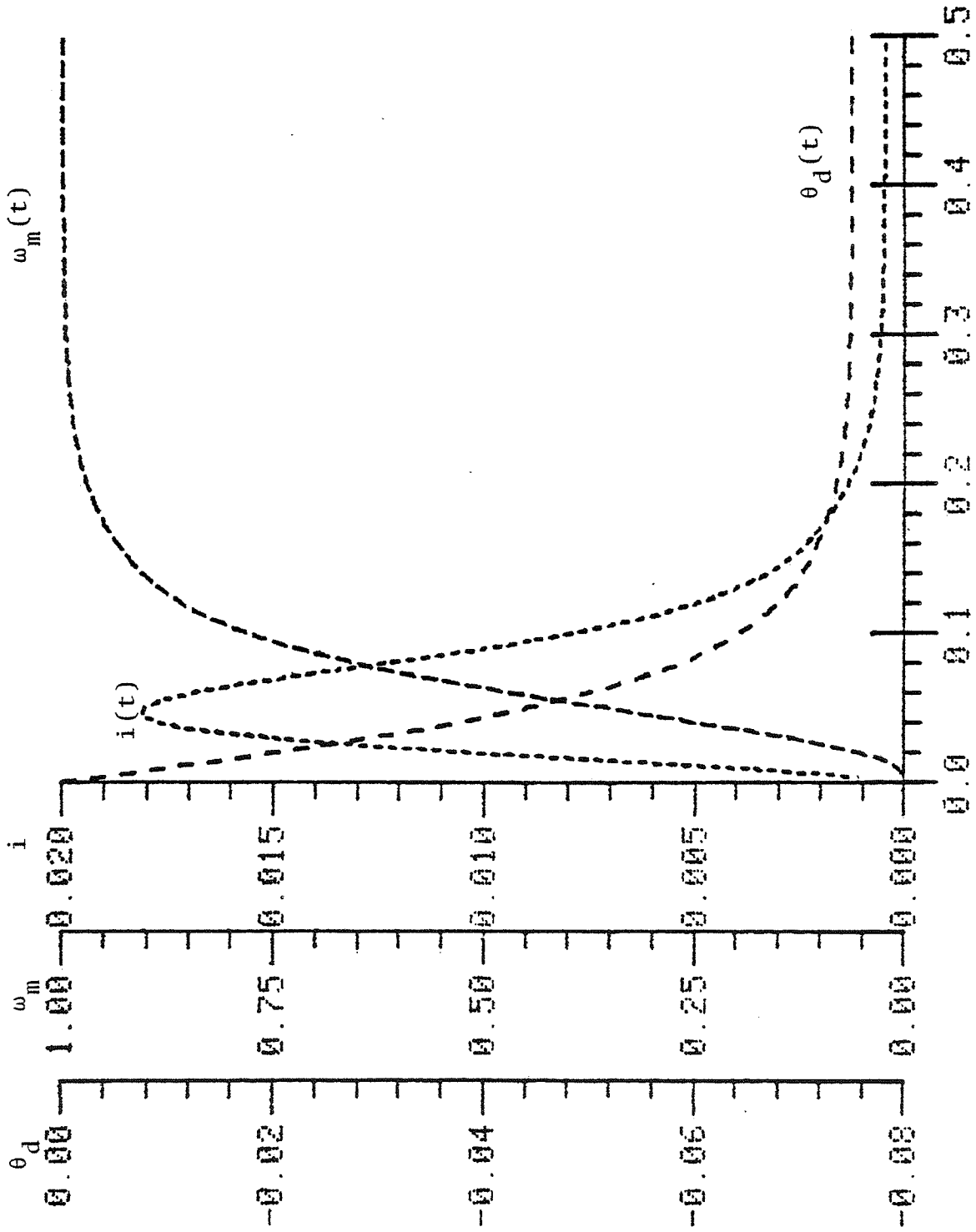


Figure C-1. Continuous-Time Closed-Loop Response of Model to a Unit-Step Input, $s_i = -20, -40+j40$.

Using $T = 0.02$ sec these poles transform to the following discrete-time poles: $z_i = 0.6703, 0.3131 \pm j0.3223$ through the transformation $z_i = e^{s_i T}$.

Given these values for z_i , and (A_d, B_d) above, LINSYS computes the feedback:

$$F_d = [7.6728 \times 10^{-1} \quad 3.3982 \times 10^{-2} \quad -1.4981]$$

The units are: $[F_d] = [V/A \quad V\text{-sec/rad} \quad V/\text{rad}]$

Observer design is accomplished in a similar way. Choose observer poles to be five times "faster" than the system:

$$s_i = -100, -200 \pm j200$$

giving $z_i = 0.1353, -0.01197 \pm j0.01386$

Given these values for z_i , and (A_d, C_d) where $C_d = [0 \ 0 \ 1]$, LINSYS computes the observer feedback matrix:

$$K_d = \begin{bmatrix} 2.7185 \times 10^{-1} \\ -1.3579 \\ 9.2024 \times 10^{-1} \end{bmatrix} \quad \text{Units: } [K_d] = \begin{bmatrix} A/\text{rad} \\ 1/\text{sec} \\ - \end{bmatrix}$$

The overall discrete-observer matrix is (see equations (55) and (56)):

$$A_{od} = \begin{bmatrix} 5.8248 \times 10^{-2} & -2.4659 \times 10^{-2} & -5.9019 \times 10^{-1} \\ 4.8639 & 3.2772 \times 10^{-1} & -7.0764 \\ 6.8342 \times 10^{-2} & 1.2859 \times 10^{-2} & -9.7100 \times 10^{-3} \end{bmatrix}$$

$$\text{Units: } [A_{od}] = \begin{bmatrix} - & \text{A-sec/rad} & \text{A/rad} \\ \text{rad/A-sec} & - & \text{1/sec} \\ \text{rad/A} & \text{sec} & - \end{bmatrix}$$

APPENDIX DSYSTEM PERFORMANCE

The performance of the velocity control system is shown in Figure D-1. Figure D-1(a) shows how the system rapidly converges to the requested velocity. There is a small amount of velocity overshoot that did not occur in the continuous-time simulation (Figure C-1). This is due to inaccuracies between the model and the physical system. These velocity measurements were made using the motor's built-in tachometer, which is why there is a ripple on the steady-state velocity.

The system's response to a varying load is seen in Figure D-1(b). At points A and C the motor was slowed down by adding friction to its shaft, but in each case the integral controller was able to correct for this and the motor resumed its original speed. Points B and D are where the extra drag was removed. The speed momentarily increased and then resumed correctly.

Responses of the simplified positioning system are shown in Figure D-2. It is slow to converge to a requested position, although its initial response is quite fast. A significant amount of ringing is produced for even the small value of C_p in Figure D-2(a). For values of C_p larger than used here, the system became unstable.

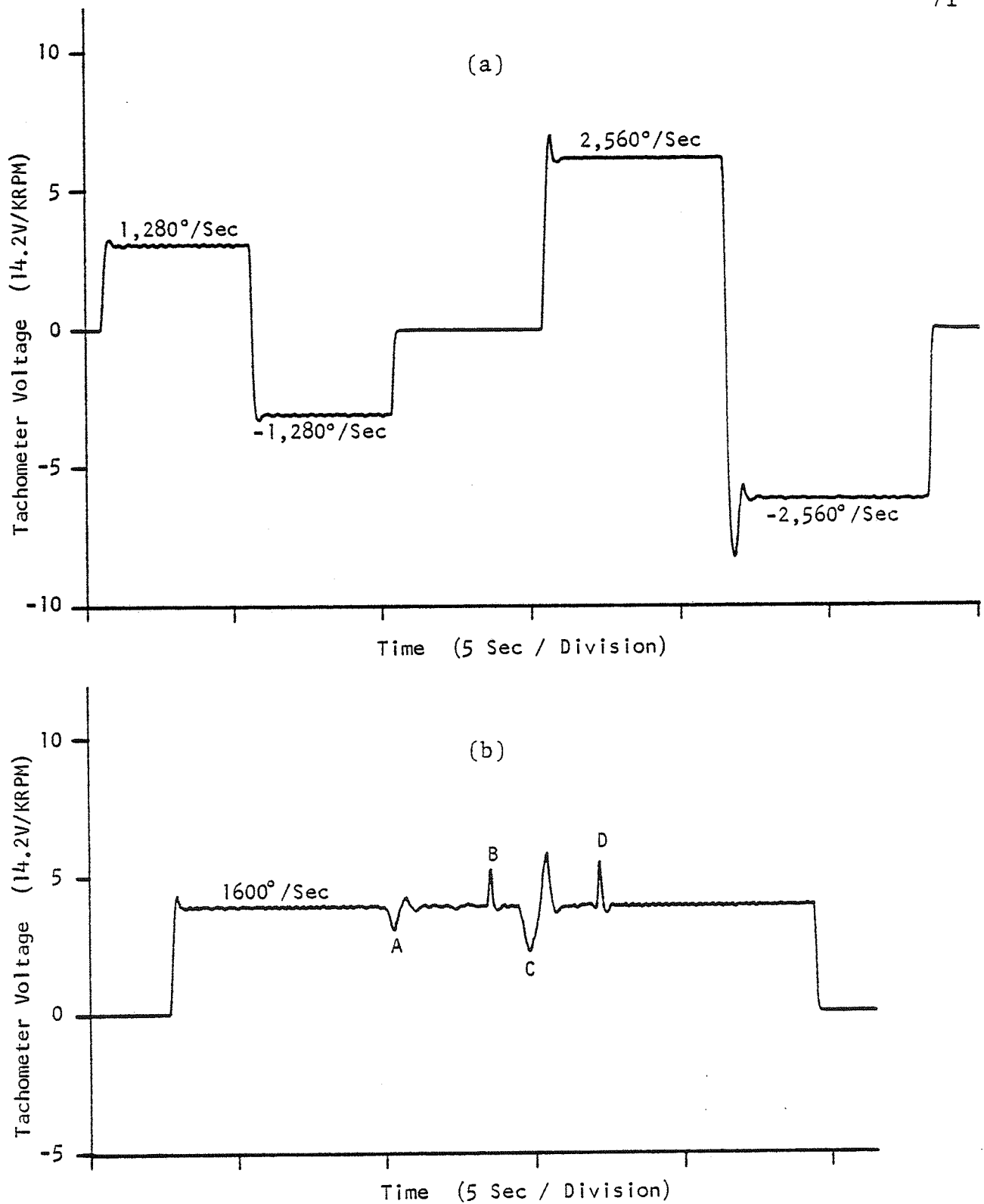


Figure D-1. Response of Velocity Controller.
(a) Step Inputs, (b) Varying Load.

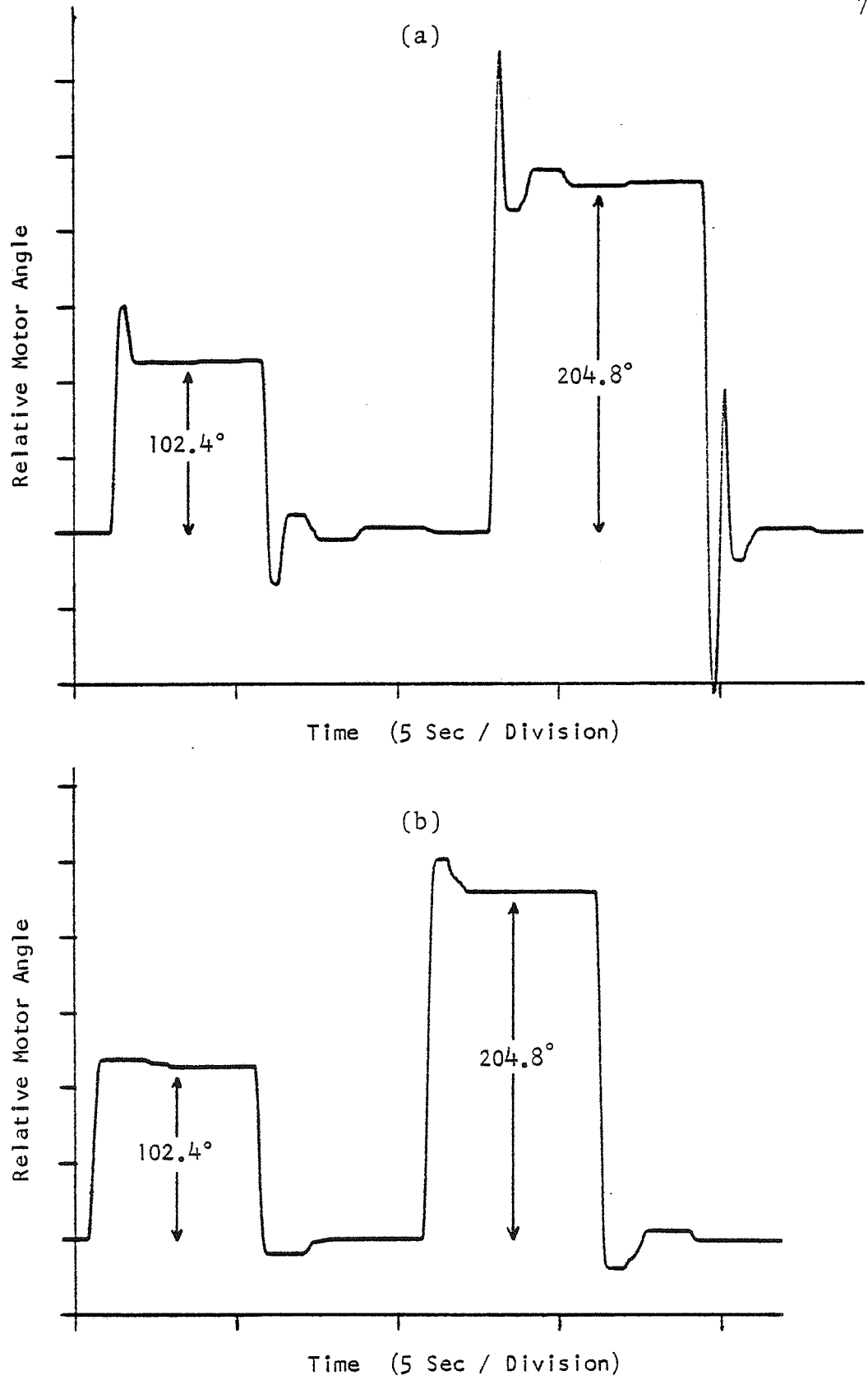


Figure D-2. Response of Simplified Position Controller to Step-Inputs. (a) $C_p = 3/16$, (b) $C_p = 2/16$.

APPENDIX EPROGRAM LISTING

CARD #	LOC	CODE	CARD
1	000		THIS FILE CONTAINS THE DEFINITIONS OF ALL SYMBOLIC NAMES AND THE ALLOCATION FOR PAGE-ZERO MEMORY.
2	001		STATE
3	002		NUMBER OF SYSTEM STATES
4	003		HIGH POSSIBLE OUTPUT VOLTS (4, 4 FORMAT, UNSIGNED).
5	004		HIGH BYTE OF THE ABOVE.
6	005		LOW BYTE OF THE ABOVE.
7	006		MASK FOR CA1 BIT IN IFR.
8	007		MASK FOR T1 BIT IN IFR.
9	008		VIA #
10	009		OUTPUT REG B, MOTOR DIRECTION CONTROL.
11	010		DATA DIRECTION REG A.
12	011		VIA #
13	012		INPUT REG B, MOTOR ANGLE; HIGH BYTE.
14	013		INPUT REG B, MOTOR ANGLE; LOW BYTE.
15	014		DATA DIRECTION REG A.
16	015		AUXILIARY CONTROL REG.
17	016		VIA #
18	017		COUNTER HIGH.
19	018		COUNTER LOW.
20	019		CONTROL FLAG REGISTER.
21	020		INTERRUPT ENABLE REGISTER.
22	021		INTERRUPT HANDLER ADDRESS.
23	022		UNWIND ADDRESS.
24	023		READ 2 HEX DIGITS FROM RAM.
25	024		READ 2 HEX DIGITS FROM RAM.
26	025		READ 2 HEX DIGITS FROM RAM.
27	026		READ 2 HEX DIGITS FROM RAM.
28	027		READ 2 HEX DIGITS FROM RAM.
29	028		READ 2 HEX DIGITS FROM RAM.
30	029		READ 2 HEX DIGITS FROM RAM.
31	030		READ 2 HEX DIGITS FROM RAM.
32	031		READ 2 HEX DIGITS FROM RAM.
33	032		READ 2 HEX DIGITS FROM RAM.
34	033		READ 2 HEX DIGITS FROM RAM.
35	034		READ 2 HEX DIGITS FROM RAM.
36	035		READ 2 HEX DIGITS FROM RAM.
37	036		READ 2 HEX DIGITS FROM RAM.
38	037		READ 2 HEX DIGITS FROM RAM.
39	038		READ 2 HEX DIGITS FROM RAM.
40	039		READ 2 HEX DIGITS FROM RAM.
41	040		READ 2 HEX DIGITS FROM RAM.
42	041		READ 2 HEX DIGITS FROM RAM.
43	042		READ 2 HEX DIGITS FROM RAM.
44	043		READ 2 HEX DIGITS FROM RAM.
45	044		READ 2 HEX DIGITS FROM RAM.
46	045		READ 2 HEX DIGITS FROM RAM.
47	046		READ 2 HEX DIGITS FROM RAM.
48	047		READ 2 HEX DIGITS FROM RAM.
49	048		READ 2 HEX DIGITS FROM RAM.
50	049		READ 2 HEX DIGITS FROM RAM.
51	050		READ 2 HEX DIGITS FROM RAM.
52	051		READ 2 HEX DIGITS FROM RAM.
53	052		READ 2 HEX DIGITS FROM RAM.
54	053		READ 2 HEX DIGITS FROM RAM.
55	054		READ 2 HEX DIGITS FROM RAM.
56	055		READ 2 HEX DIGITS FROM RAM.
57	056		READ 2 HEX DIGITS FROM RAM.
58	057		READ 2 HEX DIGITS FROM RAM.
59	058		READ 2 HEX DIGITS FROM RAM.
60	059		READ 2 HEX DIGITS FROM RAM.
61	060		READ 2 HEX DIGITS FROM RAM.
62	061		READ 2 HEX DIGITS FROM RAM.
63	062		READ 2 HEX DIGITS FROM RAM.
64	063		READ 2 HEX DIGITS FROM RAM.
65	064		READ 2 HEX DIGITS FROM RAM.
66	065		READ 2 HEX DIGITS FROM RAM.
67	066		READ 2 HEX DIGITS FROM RAM.
68	067		READ 2 HEX DIGITS FROM RAM.
69	068		READ 2 HEX DIGITS FROM RAM.
70	069		READ 2 HEX DIGITS FROM RAM.
71	070		READ 2 HEX DIGITS FROM RAM.
72	071		READ 2 HEX DIGITS FROM RAM.
73	072		READ 2 HEX DIGITS FROM RAM.
74	073		READ 2 HEX DIGITS FROM RAM.
75	074		READ 2 HEX DIGITS FROM RAM.
76	075		READ 2 HEX DIGITS FROM RAM.
77	076		READ 2 HEX DIGITS FROM RAM.
78	077		READ 2 HEX DIGITS FROM RAM.
79	078		READ 2 HEX DIGITS FROM RAM.
80	079		READ 2 HEX DIGITS FROM RAM.
81	080		READ 2 HEX DIGITS FROM RAM.
82	081		READ 2 HEX DIGITS FROM RAM.
83	082		READ 2 HEX DIGITS FROM RAM.
84	083		READ 2 HEX DIGITS FROM RAM.
85	084		READ 2 HEX DIGITS FROM RAM.
86	085		READ 2 HEX DIGITS FROM RAM.
87	086		READ 2 HEX DIGITS FROM RAM.
88	087		READ 2 HEX DIGITS FROM RAM.
89	088		READ 2 HEX DIGITS FROM RAM.
90	089		READ 2 HEX DIGITS FROM RAM.
91	090		READ 2 HEX DIGITS FROM RAM.
92	091		READ 2 HEX DIGITS FROM RAM.
93	092		READ 2 HEX DIGITS FROM RAM.
94	093		READ 2 HEX DIGITS FROM RAM.
95	094		READ 2 HEX DIGITS FROM RAM.
96	095		READ 2 HEX DIGITS FROM RAM.
97	096		READ 2 HEX DIGITS FROM RAM.
98	097		READ 2 HEX DIGITS FROM RAM.
99	098		READ 2 HEX DIGITS FROM RAM.
100	099		READ 2 HEX DIGITS FROM RAM.

BIAS VOLTAGE TO CANCEL STATIC FRICTION, 811.4 FORMAT.
MAGNITUDE OF MOTOR CONTROL SIGNAL.
SIGN OF MOTOR CONTROL SIGNAL.
POSITIONAL FEEDBACK CONSTANT.
OVERALL A-MATRIX, 815 FORMAT.

CARD #	LOC	CODE	CARD	TEXT
1	00000		AD1	WORD 0
2	00001		AD2	WORD 0
3	00002		AD3	WORD 0
4	00003		AD4	WORD 0
5	00004		AD5	WORD 0
6	00005		AD6	WORD 0
7	00006		AD7	WORD 0
8	00007		AD8	WORD 0
9	00008		AD9	WORD 0
10	00009		AD10	WORD 0
11	00010		AD11	WORD 0
12	00011		AD12	WORD 0
13	00012		AD13	WORD 0
14	00013		AD14	WORD 0
15	00014		AD15	WORD 0
16	00015		AD16	WORD 0
17	00016		AD17	WORD 0
18	00017		AD18	WORD 0
19	00018		AD19	WORD 0
20	00019		AD20	WORD 0
21	00020		AD21	WORD 0
22	00021		AD22	WORD 0
23	00022		AD23	WORD 0
24	00023		AD24	WORD 0
25	00024		AD25	WORD 0
26	00025		AD26	WORD 0
27	00026		AD27	WORD 0
28	00027		AD28	WORD 0
29	00028		AD29	WORD 0
30	00029		AD30	WORD 0
31	00030		AD31	WORD 0
32	00031		AD32	WORD 0
33	00032		AD33	WORD 0
34	00033		AD34	WORD 0
35	00034		AD35	WORD 0
36	00035		AD36	WORD 0
37	00036		AD37	WORD 0
38	00037		AD38	WORD 0
39	00038		AD39	WORD 0
40	00039		AD40	WORD 0
41	00040		AD41	WORD 0
42	00041		AD42	WORD 0
43	00042		AD43	WORD 0
44	00043		AD44	WORD 0
45	00044		AD45	WORD 0
46	00045		AD46	WORD 0
47	00046		AD47	WORD 0
48	00047		AD48	WORD 0
49	00048		AD49	WORD 0
50	00049		AD50	WORD 0
51	00050		AD51	WORD 0
52	00051		AD52	WORD 0
53	00052		AD53	WORD 0
54	00053		AD54	WORD 0
55	00054		AD55	WORD 0
56	00055		AD56	WORD 0
57	00056		AD57	WORD 0
58	00057		AD58	WORD 0
59	00058		AD59	WORD 0
60	00059		AD60	WORD 0
61	00060		AD61	WORD 0
62	00061		AD62	WORD 0
63	00062		AD63	WORD 0
64	00063		AD64	WORD 0
65	00064		AD65	WORD 0
66	00065		AD66	WORD 0
67	00066		AD67	WORD 0
68	00067		AD68	WORD 0
69	00068		AD69	WORD 0
70	00069		AD70	WORD 0
71	00070		AD71	WORD 0
72	00071		AD72	WORD 0
73	00072		AD73	WORD 0
74	00073		AD74	WORD 0
75	00074		AD75	WORD 0
76	00075		AD76	WORD 0
77	00076		AD77	WORD 0
78	00077		AD78	WORD 0
79	00078		AD79	WORD 0
80	00079		AD80	WORD 0
81	00080		AD81	WORD 0
82	00081		AD82	WORD 0
83	00082		AD83	WORD 0
84	00083		AD84	WORD 0
85	00084		AD85	WORD 0
86	00085		AD86	WORD 0
87	00086		AD87	WORD 0
88	00087		AD88	WORD 0
89	00088		AD89	WORD 0
90	00089		AD90	WORD 0
91	00090		AD91	WORD 0
92	00091		AD92	WORD 0
93	00092		AD93	WORD 0
94	00093		AD94	WORD 0
95	00094		AD95	WORD 0
96	00095		AD96	WORD 0
97	00096		AD97	WORD 0
98	00097		AD98	WORD 0
99	00098		AD99	WORD 0
100	00099		AD100	WORD 0

1 ROW 1.
 OBSERVER VECTOR, 1ST ELEMENT.
 2 ROW 2.
 OBSERVER VECTOR, 2ND ELEMENT.
 3 ROW 3.
 OBSERVER VECTOR, 3RD ELEMENT.
 4 OBSERVER VECTOR, 4TH ELEMENT.
 5 OBSERVER VECTOR, 5TH ELEMENT.
 6 OBSERVER VECTOR, 6TH ELEMENT.
 7 OBSERVER VECTOR, 7TH ELEMENT.
 8 OBSERVER VECTOR, 8TH ELEMENT.
 9 OBSERVER VECTOR, 9TH ELEMENT.
 10 OBSERVER VECTOR, 10TH ELEMENT.
 11 OBSERVER VECTOR, 11TH ELEMENT.
 12 OBSERVER VECTOR, 12TH ELEMENT.
 13 OBSERVER VECTOR, 13TH ELEMENT.
 14 OBSERVER VECTOR, 14TH ELEMENT.
 15 OBSERVER VECTOR, 15TH ELEMENT.
 16 OBSERVER VECTOR, 16TH ELEMENT.
 17 OBSERVER VECTOR, 17TH ELEMENT.
 18 OBSERVER VECTOR, 18TH ELEMENT.
 19 OBSERVER VECTOR, 19TH ELEMENT.
 20 OBSERVER VECTOR, 20TH ELEMENT.
 21 OBSERVER VECTOR, 21TH ELEMENT.
 22 OBSERVER VECTOR, 22TH ELEMENT.
 23 OBSERVER VECTOR, 23TH ELEMENT.
 24 OBSERVER VECTOR, 24TH ELEMENT.
 25 OBSERVER VECTOR, 25TH ELEMENT.
 26 OBSERVER VECTOR, 26TH ELEMENT.
 27 OBSERVER VECTOR, 27TH ELEMENT.
 28 OBSERVER VECTOR, 28TH ELEMENT.
 29 OBSERVER VECTOR, 29TH ELEMENT.
 30 OBSERVER VECTOR, 30TH ELEMENT.
 31 OBSERVER VECTOR, 31TH ELEMENT.
 32 OBSERVER VECTOR, 32TH ELEMENT.
 33 OBSERVER VECTOR, 33TH ELEMENT.
 34 OBSERVER VECTOR, 34TH ELEMENT.
 35 OBSERVER VECTOR, 35TH ELEMENT.
 36 OBSERVER VECTOR, 36TH ELEMENT.
 37 OBSERVER VECTOR, 37TH ELEMENT.
 38 OBSERVER VECTOR, 38TH ELEMENT.
 39 OBSERVER VECTOR, 39TH ELEMENT.
 40 OBSERVER VECTOR, 40TH ELEMENT.
 41 OBSERVER VECTOR, 41TH ELEMENT.
 42 OBSERVER VECTOR, 42TH ELEMENT.
 43 OBSERVER VECTOR, 43TH ELEMENT.
 44 OBSERVER VECTOR, 44TH ELEMENT.
 45 OBSERVER VECTOR, 45TH ELEMENT.
 46 OBSERVER VECTOR, 46TH ELEMENT.
 47 OBSERVER VECTOR, 47TH ELEMENT.
 48 OBSERVER VECTOR, 48TH ELEMENT.
 49 OBSERVER VECTOR, 49TH ELEMENT.
 50 OBSERVER VECTOR, 50TH ELEMENT.
 51 OBSERVER VECTOR, 51TH ELEMENT.
 52 OBSERVER VECTOR, 52TH ELEMENT.
 53 OBSERVER VECTOR, 53TH ELEMENT.
 54 OBSERVER VECTOR, 54TH ELEMENT.
 55 OBSERVER VECTOR, 55TH ELEMENT.
 56 OBSERVER VECTOR, 56TH ELEMENT.
 57 OBSERVER VECTOR, 57TH ELEMENT.
 58 OBSERVER VECTOR, 58TH ELEMENT.
 59 OBSERVER VECTOR, 59TH ELEMENT.
 60 OBSERVER VECTOR, 60TH ELEMENT.
 61 OBSERVER VECTOR, 61TH ELEMENT.
 62 OBSERVER VECTOR, 62TH ELEMENT.
 63 OBSERVER VECTOR, 63TH ELEMENT.
 64 OBSERVER VECTOR, 64TH ELEMENT.
 65 OBSERVER VECTOR, 65TH ELEMENT.
 66 OBSERVER VECTOR, 66TH ELEMENT.
 67 OBSERVER VECTOR, 67TH ELEMENT.
 68 OBSERVER VECTOR, 68TH ELEMENT.
 69 OBSERVER VECTOR, 69TH ELEMENT.
 70 OBSERVER VECTOR, 70TH ELEMENT.
 71 OBSERVER VECTOR, 71TH ELEMENT.
 72 OBSERVER VECTOR, 72TH ELEMENT.
 73 OBSERVER VECTOR, 73TH ELEMENT.
 74 OBSERVER VECTOR, 74TH ELEMENT.
 75 OBSERVER VECTOR, 75TH ELEMENT.
 76 OBSERVER VECTOR, 76TH ELEMENT.
 77 OBSERVER VECTOR, 77TH ELEMENT.
 78 OBSERVER VECTOR, 78TH ELEMENT.
 79 OBSERVER VECTOR, 79TH ELEMENT.
 80 OBSERVER VECTOR, 80TH ELEMENT.
 81 OBSERVER VECTOR, 81TH ELEMENT.
 82 OBSERVER VECTOR, 82TH ELEMENT.
 83 OBSERVER VECTOR, 83TH ELEMENT.
 84 OBSERVER VECTOR, 84TH ELEMENT.
 85 OBSERVER VECTOR, 85TH ELEMENT.
 86 OBSERVER VECTOR, 86TH ELEMENT.
 87 OBSERVER VECTOR, 87TH ELEMENT.
 88 OBSERVER VECTOR, 88TH ELEMENT.
 89 OBSERVER VECTOR, 89TH ELEMENT.
 90 OBSERVER VECTOR, 90TH ELEMENT.
 91 OBSERVER VECTOR, 91TH ELEMENT.
 92 OBSERVER VECTOR, 92TH ELEMENT.
 93 OBSERVER VECTOR, 93TH ELEMENT.
 94 OBSERVER VECTOR, 94TH ELEMENT.
 95 OBSERVER VECTOR, 95TH ELEMENT.
 96 OBSERVER VECTOR, 96TH ELEMENT.
 97 OBSERVER VECTOR, 97TH ELEMENT.
 98 OBSERVER VECTOR, 98TH ELEMENT.
 99 OBSERVER VECTOR, 99TH ELEMENT.
 100 OBSERVER VECTOR, 100TH ELEMENT.

CARD #	LOC	CODE	CARD
1	00000000	20000000	LDX #XH STATE+1
2	00000000	20000000	LDA #XH STATE+1
3	00000000	20000000	LDX #XH STATE+1
4	00000000	20000000	LDA #XH STATE+1
5	00000000	20000000	LDX #XH STATE+1
6	00000000	20000000	LDA #XH STATE+1
7	00000000	20000000	LDX #XH STATE+1
8	00000000	20000000	LDA #XH STATE+1
9	00000000	20000000	LDX #XH STATE+1
10	00000000	20000000	LDA #XH STATE+1
11	00000000	20000000	LDX #XH STATE+1
12	00000000	20000000	LDA #XH STATE+1
13	00000000	20000000	LDX #XH STATE+1
14	00000000	20000000	LDA #XH STATE+1
15	00000000	20000000	LDX #XH STATE+1
16	00000000	20000000	LDA #XH STATE+1
17	00000000	20000000	LDX #XH STATE+1
18	00000000	20000000	LDA #XH STATE+1
19	00000000	20000000	LDX #XH STATE+1
20	00000000	20000000	LDA #XH STATE+1
21	00000000	20000000	LDX #XH STATE+1
22	00000000	20000000	LDA #XH STATE+1
23	00000000	20000000	LDX #XH STATE+1
24	00000000	20000000	LDA #XH STATE+1
25	00000000	20000000	LDX #XH STATE+1
26	00000000	20000000	LDA #XH STATE+1
27	00000000	20000000	LDX #XH STATE+1
28	00000000	20000000	LDA #XH STATE+1
29	00000000	20000000	LDX #XH STATE+1
30	00000000	20000000	LDA #XH STATE+1
31	00000000	20000000	LDX #XH STATE+1
32	00000000	20000000	LDA #XH STATE+1
33	00000000	20000000	LDX #XH STATE+1
34	00000000	20000000	LDA #XH STATE+1
35	00000000	20000000	LDX #XH STATE+1
36	00000000	20000000	LDA #XH STATE+1
37	00000000	20000000	LDX #XH STATE+1
38	00000000	20000000	LDA #XH STATE+1
39	00000000	20000000	LDX #XH STATE+1
40	00000000	20000000	LDA #XH STATE+1
41	00000000	20000000	LDX #XH STATE+1
42	00000000	20000000	LDA #XH STATE+1
43	00000000	20000000	LDX #XH STATE+1
44	00000000	20000000	LDA #XH STATE+1
45	00000000	20000000	LDX #XH STATE+1
46	00000000	20000000	LDA #XH STATE+1
47	00000000	20000000	LDX #XH STATE+1
48	00000000	20000000	LDA #XH STATE+1
49	00000000	20000000	LDX #XH STATE+1
50	00000000	20000000	LDA #XH STATE+1
51	00000000	20000000	LDX #XH STATE+1
52	00000000	20000000	LDA #XH STATE+1
53	00000000	20000000	LDX #XH STATE+1
54	00000000	20000000	LDA #XH STATE+1
55	00000000	20000000	LDX #XH STATE+1
56	00000000	20000000	LDA #XH STATE+1
57	00000000	20000000	LDX #XH STATE+1
58	00000000	20000000	LDA #XH STATE+1
59	00000000	20000000	LDX #XH STATE+1
60	00000000	20000000	LDA #XH STATE+1
61	00000000	20000000	LDX #XH STATE+1
62	00000000	20000000	LDA #XH STATE+1
63	00000000	20000000	LDX #XH STATE+1
64	00000000	20000000	LDA #XH STATE+1
65	00000000	20000000	LDX #XH STATE+1
66	00000000	20000000	LDA #XH STATE+1
67	00000000	20000000	LDX #XH STATE+1
68	00000000	20000000	LDA #XH STATE+1
69	00000000	20000000	LDX #XH STATE+1
70	00000000	20000000	LDA #XH STATE+1
71	00000000	20000000	LDX #XH STATE+1
72	00000000	20000000	LDA #XH STATE+1
73	00000000	20000000	LDX #XH STATE+1
74	00000000	20000000	LDA #XH STATE+1
75	00000000	20000000	LDX #XH STATE+1
76	00000000	20000000	LDA #XH STATE+1
77	00000000	20000000	LDX #XH STATE+1
78	00000000	20000000	LDA #XH STATE+1
79	00000000	20000000	LDX #XH STATE+1
80	00000000	20000000	LDA #XH STATE+1
81	00000000	20000000	LDX #XH STATE+1
82	00000000	20000000	LDA #XH STATE+1
83	00000000	20000000	LDX #XH STATE+1
84	00000000	20000000	LDA #XH STATE+1
85	00000000	20000000	LDX #XH STATE+1
86	00000000	20000000	LDA #XH STATE+1
87	00000000	20000000	LDX #XH STATE+1
88	00000000	20000000	LDA #XH STATE+1
89	00000000	20000000	LDX #XH STATE+1
90	00000000	20000000	LDA #XH STATE+1
91	00000000	20000000	LDX #XH STATE+1
92	00000000	20000000	LDA #XH STATE+1
93	00000000	20000000	LDX #XH STATE+1
94	00000000	20000000	LDA #XH STATE+1
95	00000000	20000000	LDX #XH STATE+1
96	00000000	20000000	LDA #XH STATE+1
97	00000000	20000000	LDX #XH STATE+1
98	00000000	20000000	LDA #XH STATE+1
99	00000000	20000000	LDX #XH STATE+1
100	00000000	20000000	LDA #XH STATE+1

STORE IN XH1KPI
 STATE (XHKPI) .

CORRECTLY-SHIFTED DISTURBANCE FROM THIS STATE.

SEE IF IN POSITION-CONTROL MODE, IF SO ENTER POSITION CONTROLLER.

MOVE XHAT(K+1) TO XHAT(K) (XHKPI TO XH) .

CARD #	LUC	CODE	CARD	ASSEMBLY
4322			LPI	LPI
4323			LOX	LOX
4324			LPI	LPI
4325			LOX	LOX
4326			LPI	LPI
4327			LOX	LOX
4328			LPI	LPI
4329			LOX	LOX
4330			LPI	LPI
4331			LOX	LOX
4332			LPI	LPI
4333			LOX	LOX
4334			LPI	LPI
4335			LOX	LOX
4336			LPI	LPI
4337			LOX	LOX
4338			LPI	LPI
4339			LOX	LOX
4340			LPI	LPI
4341			LOX	LOX
4342			LPI	LPI
4343			LOX	LOX
4344			LPI	LPI
4345			LOX	LOX
4346			LPI	LPI
4347			LOX	LOX
4348			LPI	LPI
4349			LOX	LOX
4350			LPI	LPI
4351			LOX	LOX
4352			LPI	LPI
4353			LOX	LOX
4354			LPI	LPI
4355			LOX	LOX
4356			LPI	LPI
4357			LOX	LOX
4358			LPI	LPI
4359			LOX	LOX
4360			LPI	LPI
4361			LOX	LOX
4362			LPI	LPI
4363			LOX	LOX
4364			LPI	LPI
4365			LOX	LOX
4366			LPI	LPI
4367			LOX	LOX
4368			LPI	LPI
4369			LOX	LOX
4370			LPI	LPI
4371			LOX	LOX
4372			LPI	LPI
4373			LOX	LOX
4374			LPI	LPI
4375			LOX	LOX
4376			LPI	LPI
4377			LOX	LOX
4378			LPI	LPI
4379			LOX	LOX
4380			LPI	LPI
4381			LOX	LOX
4382			LPI	LPI
4383			LOX	LOX
4384			LPI	LPI
4385			LOX	LOX
4386			LPI	LPI
4387			LOX	LOX
4388			LPI	LPI
4389			LOX	LOX
4390			LPI	LPI
4391			LOX	LOX
4392			LPI	LPI
4393			LOX	LOX
4394			LPI	LPI
4395			LOX	LOX
4396			LPI	LPI
4397			LOX	LOX
4398			LPI	LPI
4399			LOX	LOX
4400			LPI	LPI
4401			LOX	LOX
4402			LPI	LPI
4403			LOX	LOX
4404			LPI	LPI
4405			LOX	LOX
4406			LPI	LPI
4407			LOX	LOX
4408			LPI	LPI
4409			LOX	LOX
4410			LPI	LPI
4411			LOX	LOX
4412			LPI	LPI
4413			LOX	LOX
4414			LPI	LPI
4415			LOX	LOX
4416			LPI	LPI
4417			LOX	LOX
4418			LPI	LPI
4419			LOX	LOX
4420			LPI	LPI
4421			LOX	LOX
4422			LPI	LPI
4423			LOX	LOX
4424			LPI	LPI
4425			LOX	LOX
4426			LPI	LPI
4427			LOX	LOX
4428			LPI	LPI
4429			LOX	LOX
4430			LPI	LPI
4431			LOX	LOX
4432			LPI	LPI
4433			LOX	LOX
4434			LPI	LPI
4435			LOX	LOX
4436			LPI	LPI
4437			LOX	LOX
4438			LPI	LPI
4439			LOX	LOX
4440			LPI	LPI
4441			LOX	LOX
4442			LPI	LPI
4443			LOX	LOX
4444			LPI	LPI
4445			LOX	LOX
4446			LPI	LPI
4447			LOX	LOX
4448			LPI	LPI
4449			LOX	LOX
4450			LPI	LPI

CARD #	LOC	CODE	CARD
00000000	000000	00	.BYT 566,MQ+1,566,MQ
00000001	000001	01	
00000002	000002	02	PCS SHIFT ; DON'T APPROX HQ IF LOW BIT IS 0
00000003	000003	03	7 FOR TEMP ; NOTE THE FACT THAT WE ARE DOING AN ADD
00000004	000004	04	.BYT 566,TEMP
00000005	000005	05	
00000006	000006	06	CLA AC ; ADD THE 2-BYTE
00000007	000007	07	ADC AC ; ACCUMULATOR.
00000008	000008	08	SLA AC+1 ;
00000009	000009	09	LDA AC+1 ;
00000010	000010	10	STC AC ;
00000011	000011	11	STC AC ;
00000012	000012	12	STC AC ;
00000013	000013	13	SHFT LDR AC ; BYTE AC RIGHT 1 BIT, PUTTING THE CORRECT SIGN IN AC(H).
00000014	000014	14	AND A TEMP ; SIGN ADJUSTED IN AC.
00000015	000015	15	ASL OR AC+1 ; ALSO SIGN PERFORMED AN ADD.
00000016	000016	16	.BYT 566,AC+1,566,AC ; CORRECT SIGN EXTENSION.
00000017	000017	17	
00000018	000018	18	DEX LOOP ; COUNT ITERATIONS
00000019	000019	19	BNE ADJUST ; AND DEPART
00000020	000020	20	FOR HQ ; FOR NEGATIVE MULTIPLIER.
00000021	000021	21	.BYT 566,MQ+1,566,MQ
00000022	000022	22	
00000023	000023	23	HCC NOSUB ; IF 8(MQ) = 0, NO NEED TO ADJUST.
00000024	000024	24	JCA AC ;
00000025	000025	25	BSTA AC+1 ;
00000026	000026	26	BBC AC+1 ;
00000027	000027	27	STC AC+1 ; SIGN OF AC IN THE FINAL SHIFT.
00000028	000028	28	ASL OR AC ;
00000029	000029	29	.BYT 566,AC+1,566,AC ;
00000030	000030	30	
00000031	000031	31	.BYT 566,MQ+1,566,MQ
00000032	000032	32	
00000033	000033	33	HTB

CARD #	LOC	CODE	AND	OPERATION	COMMENT
0000	0000	0000	STF	THER	0 THREE - THM
0001	0001	0001	THM	THM	
0002	0002	0002	THM	THM	
0003	0003	0003	THM	THM	
0004	0004	0004	THM	THM	
0005	0005	0005	THM	THM	
0006	0006	0006	THM	THM	
0007	0007	0007	THM	THM	
0008	0008	0008	THM	THM	
0009	0009	0009	THM	THM	
0010	0010	0010	THM	THM	
0011	0011	0011	THM	THM	
0012	0012	0012	THM	THM	
0013	0013	0013	THM	THM	
0014	0014	0014	THM	THM	
0015	0015	0015	THM	THM	
0016	0016	0016	THM	THM	
0017	0017	0017	THM	THM	
0018	0018	0018	THM	THM	
0019	0019	0019	THM	THM	
0020	0020	0020	THM	THM	
0021	0021	0021	THM	THM	
0022	0022	0022	THM	THM	
0023	0023	0023	THM	THM	
0024	0024	0024	THM	THM	
0025	0025	0025	THM	THM	
0026	0026	0026	THM	THM	
0027	0027	0027	THM	THM	
0028	0028	0028	THM	THM	
0029	0029	0029	THM	THM	
0030	0030	0030	THM	THM	
0031	0031	0031	THM	THM	
0032	0032	0032	THM	THM	
0033	0033	0033	THM	THM	
0034	0034	0034	THM	THM	
0035	0035	0035	THM	THM	
0036	0036	0036	THM	THM	
0037	0037	0037	THM	THM	
0038	0038	0038	THM	THM	
0039	0039	0039	THM	THM	
0040	0040	0040	THM	THM	
0041	0041	0041	THM	THM	
0042	0042	0042	THM	THM	
0043	0043	0043	THM	THM	
0044	0044	0044	THM	THM	
0045	0045	0045	THM	THM	
0046	0046	0046	THM	THM	
0047	0047	0047	THM	THM	
0048	0048	0048	THM	THM	
0049	0049	0049	THM	THM	
0050	0050	0050	THM	THM	
0051	0051	0051	THM	THM	
0052	0052	0052	THM	THM	
0053	0053	0053	THM	THM	
0054	0054	0054	THM	THM	
0055	0055	0055	THM	THM	
0056	0056	0056	THM	THM	
0057	0057	0057	THM	THM	
0058	0058	0058	THM	THM	
0059	0059	0059	THM	THM	
0060	0060	0060	THM	THM	
0061	0061	0061	THM	THM	
0062	0062	0062	THM	THM	
0063	0063	0063	THM	THM	
0064	0064	0064	THM	THM	
0065	0065	0065	THM	THM	
0066	0066	0066	THM	THM	
0067	0067	0067	THM	THM	
0068	0068	0068	THM	THM	
0069	0069	0069	THM	THM	
0070	0070	0070	THM	THM	
0071	0071	0071	THM	THM	
0072	0072	0072	THM	THM	
0073	0073	0073	THM	THM	
0074	0074	0074	THM	THM	
0075	0075	0075	THM	THM	
0076	0076	0076	THM	THM	
0077	0077	0077	THM	THM	
0078	0078	0078	THM	THM	
0079	0079	0079	THM	THM	
0080	0080	0080	THM	THM	
0081	0081	0081	THM	THM	
0082	0082	0082	THM	THM	
0083	0083	0083	THM	THM	
0084	0084	0084	THM	THM	
0085	0085	0085	THM	THM	
0086	0086	0086	THM	THM	
0087	0087	0087	THM	THM	
0088	0088	0088	THM	THM	
0089	0089	0089	THM	THM	
0090	0090	0090	THM	THM	
0091	0091	0091	THM	THM	
0092	0092	0092	THM	THM	
0093	0093	0093	THM	THM	
0094	0094	0094	THM	THM	
0095	0095	0095	THM	THM	
0096	0096	0096	THM	THM	
0097	0097	0097	THM	THM	
0098	0098	0098	THM	THM	
0099	0099	0099	THM	THM	

END OF M08/TECHNOLOGY 650X ASSEMBLY VERSION 7.0
NUMBER OF ERRORS 0, NUMBER OF WARNINGS 0

VBIA9	0020	529	322	335	342	345	
VCMULT	0021	453	323	400	408	415	
VOUTLP	0022	152	373	370	404	416	
XHKP1	0023	152	154	170	173	204	207
XHI	0024	0	401				210
XHKP1	0025	0	401				217

SYMBOL		LINE DEFINED		CROSS-REFERENCES	
XH2	0042	76	307	309	
XH3	0043	84	409		
XH3	0044	77	431		
XH3	0050	85	431		
XH3	0050	74	409	397	405
XH3	0050	233	230		413
XH3	0050				455

REFERENCES

1. Greenleaf, J. F., Johnson, S. A., Lee, S. L., Herman, G. T., and Wood, E. H. (1974) Algebraic reconstruction of spatial distributions of acoustic absorption within tissue from their two-dimensional acoustic projections. Acoustical Holography, (Philip S. Green, editor) Plenum Press, New York, 5, 591-603.
2. Greenleaf, J. F., Johnson, S. A., Samayoa, W. F., and Duck, F. A. (1975) Algebraic reconstruction of spatial distributions of acoustic velocities in tissue from their time-of-flight profiles. Acoustical Holography (Newell Booth, editor), Plenum Press, New York, 6, 71-90.
3. Greenleaf, J. F., and Johnson, S. A. (1975) Algebraic reconstruction of spatial distribution of acoustic speed and attenuation in tissues from time-of-flight and amplitude profiles. Proceedings, Seminar on Ultrasonic Tissue Characterization, NBS Special Publication 453, Gaithersburg, Maryland, May 28-30, pp. 109-110.
4. Greenleaf, J. F., Johnson, S. A. Samayoa, W. F., and Hansen, C. R. (1976) Refractive index by reconstruction: use to improve compound B-scan resolution. Proceedings, Seventh International Symposium on Acoustical Holography and Imaging, (L. W. Kessler, editor), Plenum Press, New York, 7, 263-273.
5. MOS Technology, Inc., MCS6500 Microcomputer Family Programming Manual, MOS Technology, Inc., 1975.
6. Synertek Systems Corporation, SYM Reference Manual, Synertek Systems Corporation, Santa Clara, California, 1975.
7. Kuo, B. C., Automatic Control Systems, 3rd Edition, Prentice-Hall, Inc., Englewood Cliffs, New Jersey, 1975.
8. Bingulac, S., "Linsys Conversational Software for Analysis and Design of Linear Systems", Report T-17, Coordinated Science Laboratory, University of Illinois, Urbana, Illinois, June, 1975.
9. Electro-Craft Corporation, DC Motors, Speed Controls, Servo Systems, 4th Edition, Electro-Craft Corporation, Hopkins, Minnesota, July, 1978.
10. International Business Machines Corporation, Continuous Systems Modelling Program III (CSMP III) Program Reference Manual, Program Number 5734-X59, Publication No. SH19-7001-3, December, 1975.

11. Electro-Craft Corporation, Product Catalog, Electro-Craft Corporation, Hopkins, Minnesota, p. 76.